Appendices

Biologically Based Dose Response Models for the Effect of Perchlorate on Thyroid Hormones in the Infant, Breast Feeding Mother, Pregnant Mother, and Fetus: Model Development, Revision, and Preliminary Dose-Response Analyses

Paul Schlosser[1], Teresa Leavens[2], and Santhini Ramasamy[3]

[1] U.S. EPA, National Center for Environmental Assessment, Washington, DC

[2] PK Consultant, Cary, NC

[3] U.S. EPA, Office of Water, Washington, DC

Other contributors: Jeff Fisher[4], Annie Lumen[4], and Eva McLanahan[5,*]

[4] U.S. FDA, National Center for Toxicological Research, Jefferson, AR

[5] U.S. EPA, National Center for Environmental Assessment, Research Triangle Park, NC

*Current affiliation: Centers for Disease Control and Prevention, Agency for Toxic Substances and Disease Registry, Atlanta, GA

NOTICE

This document is a **Public Review draft.** This information is distributed solely for the purpose of pre-dissemination peer review under applicable information quality guidelines. It has not been formally disseminated by EPA. It does not represent and should not be construed to represent any Agency determination or policy. It is being circulated for review of its technical accuracy and science policy implications.

Contents

Appendix A: Parameter Definitions 3
Appendix B: Model Structure Changes and Additional Evaluation 6
B-1: Alignment of Perchlorate-NIS Affinity Values 6
B-2: Update in Affinity of Perchlorate for the Sodium-Iodide Symporter (NIS) Based on Predictions for the "Average Adult" Perchlorate/Iodide PBPK Model and In Vitro NIS Kinetics 7
B-3: Comparison of Lactating Mother BBDR Model to Greer et al. (2002) Data 12
B-4: Calibration of Vmax for Transfer of Perchlorate into Breast Milk 14
Appendix C: Supplemental Analyses of Differences among the Lactating Mother, Breast Fed Infant, and Formula Fed Infant 17
Appendix D: Perchlorate Clearance Analysis 20
Appendix E: Population Percentiles for fT4 During Pregnancy 24
References for Appendices A-E 26
Appendix F: Summary of fT4 Levels in Lactating, Pregnant, and All Other Women Based on NHANES 2007-2012 28
Method for Analyzing NHANES Data 28
Results 29
References for Appendix F 32
Appendix G: Thyroid Hormone Model Equations 34
Pregnant Mother 34
Fetus 35
Lactating Mother 35
Infant 36

Appendix A: Parameter Definitions

PARAMETER		DEFINITION
Maternal	Infant	
(n/a)	IABODY_NI	Birth amount of iodide in rest of body
AT3_T0	AT3_NT0	Initial amt. of T3 in distribution volume
AT4_T0	AT4_NT0	Initial amt. of T4 in distribution volume
IATGI	IATGI_N	Initial thyroidal organified iodide stores
CTGIPOOL	CTGIPOOL_N	Euthyroid organified iodide stores
BWPRE	BW_N0	Pre-pregnancy body weight; initial infant BW
(n/a)	BW_SENS_N	SC for body weight over time
CLUX_SENS*	CLUXC_NI_SENS*, CLUXC_NP_SENS*	SC for urinary clearance of iodide in mother and infant, and for perchlorate in infant
CLUC_P	(n/a)	Scaled urinary clearance rate for perchlorate
CLFECEST3C	CLFECEST3C_N	Fecal clearance of T3
CLFECESFT4C	CLFECEST4C_N	Fecal clearance of T4
CLMILKT3C	(n/a)	Clearance of T3 to milk
CLMILKFT4C	(n/a)	Clearance of T4 to milk
CLUT3C	(n/a)	Scaled urinary clearance of T3
CLUFT4C	CLUFT4C_N	Scaled urinary clearance of T4
FRCONVT4	FRCONVT4_N	Ratio of free T4 to total T4
IABIND_P	IABIND_NP	Initial amount of bound perchlorate in plasma
IAF_P	IAF_NP	Initial amt. of fat perchlorate
IAG_P	IAG_NP	Initial amt. of gastric tissue perchlorate
IAGB_P	IAGB_NP	Initial amt. of gastric plasma perchlorate
IAGJ_P	IAGJ_NP	Initial amt. of gastric juice perchlorate
IAK_P	IAK_NP	Initial amt. of kidney perchlorate
IAL_P	IAL_NP	Initial amt. of liver perchlorate
IAMB_I, IAMB_P	(n/a)	Initial amt. of mammary blood iodide, perchlorate
IAMK_I, IAMK_P	(n/a)	Initial amt. of milk iodide, perchlorate
IAPLAS_I, IAPLAS_P	IAPLAS_NI, IAPLAS_NP	Initial plasma iodide, FREE (unbound) perchlorate
IAR_I, IAR_P	(n/a), IAR_NP	Initial amt. of richly perfused iodide, perchlorate
IARBC_P	IARBC_NP	Initial amt. of red blood cell perchlorate
IAS_I, IAS_P	(n/a), IAS_NP	Initial amt. of slowly perfused iodide, perchlorate
IASK_P	IASK_NP	Initial amt. of skin tissue perchlorate
IASKB_P	IASKB_NP	Initial amt. of skin plasma perchlorate
IAT_FI	IAT_NFI	Initial amount of FREE thyroid iodide
IAT_P	IAT_NP	Initial amt. of thyroid tissue perchlorate
IATB_I, IATB_P	IATB_NI, IATB_NP	Initial amt. of thyroid plasma iodide, perchlorate
(n/a)	INGEST_SENS*	Sensitivity constant for ingested volume of formula (VFORMULAC) or breast milk (KTRANS)
KBINDC_I	KBINDC_NI	2nd order rate constant for organification of free iodide in thyroid

Maternal parameter	Infant parameter	Definition
KMETT3C	CLMETT3CX_SENS_N	1st order(mom) T3 degradation rate; SC infant clearance(CLMETT3CX_N)
KMETT4C	CLMETT4CX_SENS_N	1st order (mom) T4 degradation rate; SC infant clearance (CLMETT4CX_N)
KM_BPNG	KM_BNPNG	Michaelis Menten (M-M) constant for plasma binding
KM_GPNG	KM_GNPNG	M-M constant for gastric uptake (set = KM_TPNG)
KM_MKI, KM_MKPNG	(n/a)	M-M constant for iodide, perchlorate uptake into milk = KM_TPNG)
KM_SPNG	KM_SNPNG	M-M constant for skin NIS transport (= KM_TPNG)
KMTHY_I, KM_TPNG	KMTHY_NI, KM_TNPNG	M-M constant for NIS iodide, perchlorate transport in thyroid
KPRODT3C	VPRODT3F_N	1st order rate constant for production of T3; ratio of T3:T4 production in infant* VPRODT3F = VPRODT3F_N* VPRODT4CX(t)*BW_N
KPRODT4C	VPRODT4CX_SENS_N*	1st order rate constant for production of T4; SC for infant zero order T4 production (VPRODT4CX_N)
KUNBC_P	KUNBC_NP	Diffusion rate constant for perchlorate from bound compartment to plasma
PATHYC_I, PATC_P	PATHYC_NI, PATC_NP	Scaled permeability-surface area (PA) product for iodide, perchlorate diffusion between thyroid blood and thyroid tissue
PAGC_P	PAGC_NP	PA product between GI blood and tissue
PAGJC_P	PAGJC_NP	PA product for perchlorate between gastric tissue and gastric juice
PAMKC_I, PAMKC_P	(n/a)	PA product for iodide, perchlorate between milk and mammary plasma
PARBCC_P	PARBCC_NP	PA product for perchlorate into red blood cells
PASKC_P	PASKC_NP	PA product for perchlorate into skin
(n/a)	PBODY_NI	Rest of body tissue: plasma partition coefficient (PC) for iodide
PF_P	PF_NP=PF_P	Fat tissue: plasma partition PC for perchlorate
PG_P	PG_NP	Gastric tissue: plasma PC for perchlorate
PGJ_P	PGJ_NP	Gastric juice: tissue PC for perchlorate
PK_P	PK_NP=PK	Kidney: plasma PC for perchlorate
PL_P	PL_NP = PL_P	Liver: plasma PC for perchlorate
PMK_I, PMK_P	(n/a)	Milk: mammary plasma PC for iodide, perchlorate
PRP_I , PR_P	(n/a),PR_NP = PR_P	Richly perfused: plasma PC for perchlorate, iodide
PRBC_P	PRBC_NP = PRBC_P	Red blood cells: plasma PC for perchlorate
PSP_I , PS_P	(n/a), PS_NP = PS_P	Slowly perfused: plasma PC for perchlorate, iodide
PSK_P	PSK_NP = PSK_P	Skin: plasma PC for perchlorate
PTHY_I, PT_P	PTHY_NI, PT_NP=PT_P	Thyroid tissue: plasma PC for iodide, perchlorate
QCC	QCC_SENS_N*	Scaled cardiac output; SC for absolute cardiac output
QFC	(QFC*VFC_N/VFC)	Fractional plasma flow to fat

Maternal parameter	Infant parameter	Definition
QGC	(QGC*VGC_N/VGC)	Fractional plasma flow to gastric tissue
QKC	(QKC*VKC_N/VKC)	Fractional plasma flow to kidney
QLC	(QLC*VLC_N/VLC)	Fractional plasma flow to liver
QMC	(n/a)	Fractional plasma flow to mammary gland
QRC	QRC_N	Fractional plasma flow to richly perfused
QSC	QSC_N	Fractional plasma flow to slowly perfused
QSKC	(QSKC*VSKC_N/VSKC)	Maternal fractional plasma flow to skin
QTC	QTC_N	Fractional plasma flow to thyroid
T3FRAC	T3FRAC_SENS_N*	Fraction of T4 metabolized to T3, SC (T3FRAC _N)
(n/a)	VBODYC_N	Rest of body volume fraction
VDT3C	VDT3C_N	Fractional volume of distribution for T3
VDT4C	VDT4C_N	Fractional volume of distribution for T4
VF_SENS*	VF_SENS_N*	Fat volume fraction SC
VFC	(n/a)	Fat volume fraction in nonpregnant, non-lactating
VGBC	VGBC_N	GI blood (plasma + blood cells) volume fraction
VGC	VGIT_SENS_N*	GI tissue volume fraction (*SC)
VGJC	VGJC	Gastric juices volume fraction
VKC	VK_SENS_N*	Kidney volume fraction (*SC)
VLC	VL_SENS_N*	Liver volume fraction (*SC)
VMAM_SENS*	(n/a)	Mammary tissue volume SC (VmamC)
VMAXC_BP	VMAXC_BNP	Scaled Vmax for blood binding of perchlorate
VMAXC_GP	VMAXC_GNP	Scaled Vmax for NIS (active uptake of): perchlorate into gastric juice
VMAXMK_SENS	(n/a)	SC for scaled Vmax for NIS: iodide into milk (VMAXCx_MKI)
VMAXC_MKP	(n/a)	Scaled Vmax for NIS: perchlorate into milk
VMAXC_SP	VMAXC_SNP	Scaled Vmax for NIS: perchlorate into skin
VMAXC_TP	(n/a)	Scaled Vmax for NIS: perchlorate into thyroid
VMAXTHYX_SENS*	VMAXTHYX_SENS_N*	SC for NIS: iodide into thyroid (VMAXTHYCx in mother; VMAXTHYCx_N in infant) - also assesses Vmax for perchlorate in infant because VMAXTNP = VMAXTHY_NI/25
VMBC	(n/a)	Mammary gland blood fraction
VMK	(n/a)	Volume of milk
VPLASC	VPLASC_N	Plasma volume fraction
VRC	VR_SENS_N*	Richly perfused volume fraction (remaining), SC
VRBCC	VRBCC_N	Red blood cells in body volume fraction
VSC	VS_SENS_N*	Slowly perfused tissues volume fraction, SC
VSKC	VSK_SENS_N*	Skin volume fraction, SC
VSKBC	VSKBC_N	Skin blood (plasma +blood cells) volume fraction
VTBC	VTBC_N	Thyroid blood (plasma + cells) volume fraction
VTTOTC	VTHY_SENS_N*	Total thyroid volume fraction, SC
VURINE	VURINE_SENS_N*	Daily urine volume, SC for infant urine volume

* Constant multiplier with a value of one, except when used to assess sensitivity coefficients for parameters specified as table function or calculated as equation.

Appendix B: Model Structure Changes and Additional Evaluation

In developing the current iodide BBDR model for the lactating mother and infant, Dr. Fisher made two structural changes that required parallel changes in the perchlorate PBPK model for consistency. First, the lumen compartment was removed from the thyroid sub-model; in the previous models there was active transport of iodide and perchlorate from the thyroid follicle/tissue to the lumen and passive diffusion between them, so the lumen acted as a storage compartment for inorganic iodide. While it is known that a separate lumen compartment exists in the thyroid with active transport as in the previous model, Dr. Fisher deemed this to be an unnecessary complication of the model.

Second, the transfer of iodide and perchlorate into breast milk had previously been described as a two-step process: 1) transport from mammary blood plasma to mammary tissue and 2) transport from mammary tissue to the milk gland. While biological data has shown that the mammary gland actively concentrates iodide in milk by transporters that can be inhibited by perchlorate, the cellular location (apical versus basolateral) is not certain (Rillema and Hill, 2003a, b; Perron et al., 2001; Rillema et al., 2000; Brown-Grant, 1961, 1957); therefore transport was simplified in the model to occur directly from mammary blood plasma to the milk.

Along with these structural changes, the blood flow to the mammary was changed to the average rate measured by Geddes et al. (2012), and the Vmax and permeability-area diffusion constant (PAMKC_I) for iodide transfer into milk adjusted to better describe iodide dosimetry in lactating mothers and breast-fed infants. In particular PAMKC_I was reduced from 0.002 to 0.001 L/h/kg$^{0.75}$, which allowed for a greater difference between milk and plasma concentration of iodide to be obtained, hence higher iodide transfer to the infant.

As indicated above, the perchlorate PBPK model structure was therefore changed in parallel to match the iodide model structure. After making these changes, it was not clear if the previous tuning of the perchlorate model to match human perchlorate-exposure radio-iodide data (Greer et al., 2002) or breast milk data still held. Also, preliminary results with the lactating mother/breastfeeding infant model indicated that higher levels of perchlorate than previously considered could be reasonably safe, but performance of the model at these higher exposure levels had not been evaluated. The following sections describe current analyses with the model and resulting updates in parameter values made to address these concerns.

B-1: Alignment of Perchlorate-NIS Affinity Values

The perchlorate PBPK sub-model used in conjunction with the iodide/thyroid hormone (TH) BBDR model was developed in a series of steps and extrapolations, beginning with the adult male rat (Merrill et al., 2003), the lactating maternal rat and neonate (Clewell et al., 2003a), the adult "average" human (Merrill et al., 2005), and the human "Life Stage" model, which included lactation (Clewell et al., 2007). In Merrill et al. (2003) the Km for perchlorate binding to NIS ($Km_{NIS,ClO4}$; 1/affinity) was given virtually the same value for thyroid, skin, and GI tissues, 1.7 or 1.8 x 10^5 ng/L.

For the rat lactation model, Clewell et al. (2003a) adjusted these values somewhat, beginning with the Km as reported by Kosugi et al. (1996), 1.5 x 10^5 ng/L. The text of that paper states, "This value was adjusted slightly to obtain the best fit of thyroid perchlorate to the drinking water data, resulting in a Km of 2.0 x 10^5 ng/L." However in the code as obtained from Dr. Harvey Clewell the thyroid $Km_{NIS,ClO4}$ still

had a value of 1.5 x 10^5 ng/L while that for skin, GI tract, and mammary tissue was 2.0 x 10^5 ng/L. Considering that the evaluation by Kosugi et al. (1996) was in a cellular environment not native to the molecule (i.e., Chinese hamster ovarian cells in culture), it is not surprising that some adjustments were required to match the rat PK data. However this adjustment is inconsistent with the almost identical values across tissues that did fit the dosimetry in the adult male rat (Merrill et al., 2003), given just above. The molecular form of NIS would not be altered by pregnancy or lactation, while other parameters such as permeability and the partition coefficient, which depend on tissue thickness and lipid content, respectively, would be much more likely to change. Thus we suggest here that the differential adjustment of $Km_{NIS,ClO4}$ for the lactating rat may not have been necessary to fit the perchlorate PK data.

Even if adjustment of $Km_{NIS,ClO4}$ to match rat lactation data may have been appropriate, it is not clear that using different values for $Km_{NIS,ClO4}$ in different tissues is appropriate for human predictions. In particular the U.S. EPA questions use of a higher value for transfer to breast milk and competition with iodide in that process, when the Km for *iodide* on NIS is assumed to be the same for transfer to breast milk as for uptake into thyroid. The extrapolation of the difference in perchlorate $Km_{NIS,ClO4}$-values from the Clewell et al. (2003a) rat lactation model is also questionable because the current model structure no longer matches that model. Lastly, this choice results in a lower estimated effect on the breast-fed infant than assuming equality of $Km_{NIS,ClO4}$ for milk and thyroid transfer (i.e., that the milk transfer $Km_{NIS,ClO4}$ is as low as the thyroid value). Therefore, for use in EPA's analysis, $Km_{NIS,ClO4}$ was given a common value in all tissues of the lactating mother and infant models. Since the molecular form of NIS is the same across the tissues in which it is expressed, the Km for perchlorate should also be the same.

The value of $Km_{NIS,ClO4}$ for the GI tract and skin are not expected to significantly impact model predictions at or near steady-state, but given the change in value considered in the next section, it seemed appropriate and easiest to set all values the same prior to any adjustment in the thyroidal value.

Like the lactation model, the Clewell et al. (2007) pregnancy model used a lower $Km_{NIS,ClO4}$ for the maternal and fetal thyroid (1.6 x 10^5 ng/L) than other tissues (2 x 10^5 ng/L). Since the end-of-pregnancy analysis is conducted at steady-state, values of $Km_{NIS,ClO4}$ for the skin and GI tract will have little or no effect on risk predictions. For the pregnant rat Clewell et al. (2003b) used identical values for $Km_{NIS,ClO4}$ in all tissues. Thus any data from the rat on disposition of perchlorate across the rat placenta vs. thyroid do not indicate a differential value of $Km_{NIS,ClO4}$ from the thyroid. Therefore, for human predictions it again seems appropriate to assume consistency, equality of $Km_{NIS,ClO4}$ across all tissues of the pregnant mother and fetus, and in particular to use the value for the adult thyroid, whose value can be evaluated against predictions of iodide uptake inhibition in adult humans, as described next.

B-2: Update in Affinity of Perchlorate for the Sodium-Iodide Symporter (NIS) Based on Predictions for the "Average Adult" Perchlorate/Iodide PBPK Model and In Vitro NIS Kinetics

The analysis and conclusions described here have now also been reported by Schlosser (2016).

The original models for perchlorate and iodide dosimetry, and the initial effect of perchlorate, iodide uptake inhibition, from which the other life-stages and subsequent modeling have largely been extrapolated, was that of Merrill et al. (2005) for an "average" human adult, which should be predictive of healthy young men and women, outside of pregnancy and lactation. The previous evaluation of this model (U.S. EPA, 2009) focused on results at the then-established reference dose (RfD), for which the point-of-departure (POD) was the dose of 7 µg/kg/d, at which Greer et al. (2002) observed radio-iodide uptake (RAIU) of 98.2 ± 8.3% of controls. The Greer et al. (2002) data set is of primary importance because controlled perchlorate exposures were administered to a set of human volunteers and the

impact on radio-iodide uptake by the subjects' thyroids was measured during and after the 2-week exposure. Thus it provides a direct observation of this key initial endpoint in humans with known exposure levels. Hence the ability of the model to fit these data is considered an important validation measure.

The Merrill et al. (2005) model recapitulated the effect measured by Greer et al. (2002) at 7 µg/kg/d exactly, predicting radio-iodide uptake at 98.2% of control, as shown in Figure B-1. The U.S. EPA did make several minor modifications to the Merrill et al. (2005) model (described in U.S. EPA (2009)), and the results shown here and below are with that modified model. Therefore, for accuracy, it is henceforth referred to as the EPA model (U.S. EPA, 2009).

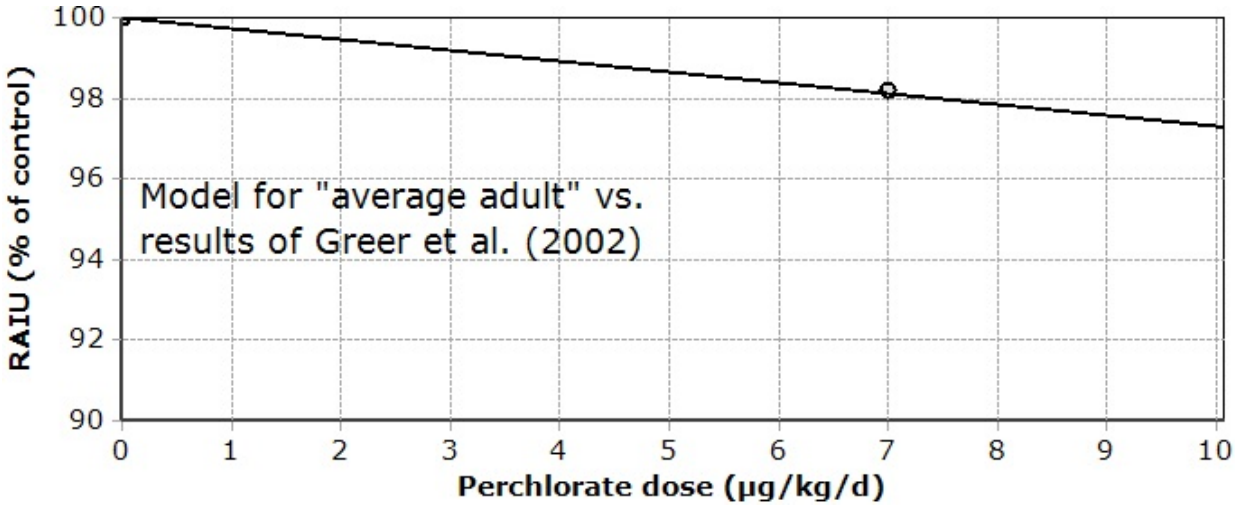

Figure B-1: Predicted low-dose Radio-Iodide Uptake (RAIU) as a % of control using the EPA perchlorate PBPK model (**U.S. EPA, 2009**) for the average adult (line) with lowest data point from **Greer et al. (2002)**. Simulation and measurement are for the last day of a two-week human study.

The prior review, however, did not evaluate model behavior at higher doses because the focus was on doses below the POD (7 µg/kg/d). With the predictions of the new BBDR modeling indicating that response of T3 and T4 might not be significant at 7 µg/kg/d, the U.S. EPA (2009) model has now been compared to the higher-dose Greer et al. (2002) data, since it is a basis for the current model: Figure B-2. The results show that the model significantly under-predicts the effect (over-predicts the RAIU as % of control) at the next two higher doses. That the prior EPA review failed to evaluate the full dose-response range and recognize the model's failure in this regard was an oversight.

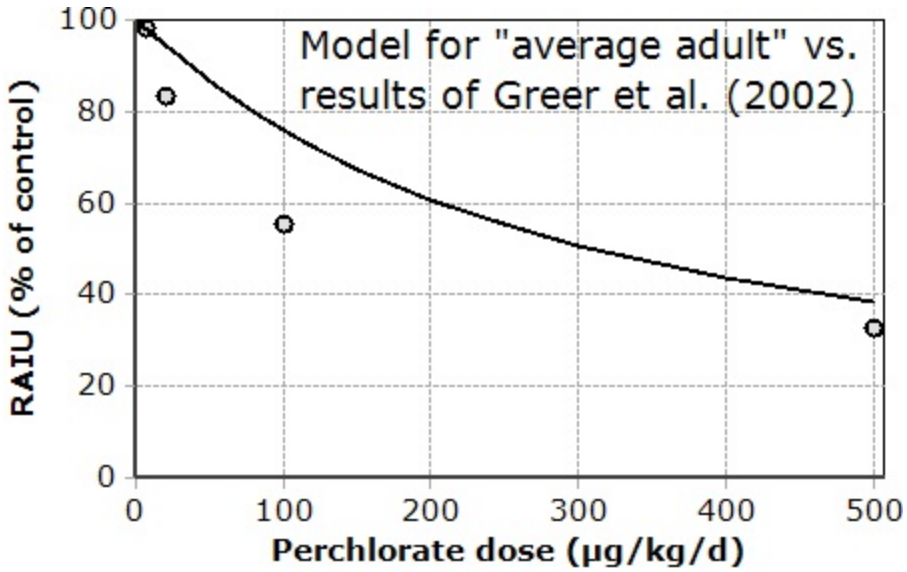

Figure B-2: Predicted Radio-Iodide Uptake (RAIU) as a % of control using the **U.S. EPA (2009)** perchlorate PBPK model for the average adult (line) with data from **Greer et al. (2002)** for all dose levels. Simulation and measurement are for the last day of a two-week human study.

To understand why this failure in prediction occurs, the ability of the U.S. EPA (2009) model to predict the blood perchlorate levels in the Greer et al. (2002) study was evaluated. While the perchlorate blood levels were not matched exactly, the difference between model predictions and measured perchlorate blood levels in the study subjects were not sufficient to explain the discrepancy in fits to RAIU inhibition shown above (results not shown). Since blood perchlorate levels were predicted reasonably well, the next most important parameter which might explain this discrepancy is the affinity of perchlorate for the NIS, $Km_{NIS,ClO4}$, which is central to the prediction of iodide uptake.

As described above, $Km_{NIS,ClO4}$ had been given a value of $1.6x10^5$ ng/L by Merrill et al. (2005) based on an in vitro study by Kosugi et al. (1996), who expressed *rat* NIS in Chinese hamster ovary (CHO) cells. Given that the results of Kosugi et al. (1996) were for a non-human form of NIS expressed outside of its normal tissue and cellular environment, it is possible that the measured affinity might not be exactly predictive of the effects of perchlorate in humans. Initial tests with the U.S. EPA (2009) adult human model indicated that increasing the affinity (reducing the Km) about 3-fold would provide a better fit to the data. Thus, simply re-fitting the Km to the human *in vivo* data seemed justified.

However, we first examined the manner in which Kosugi et al. (1996) estimated $Km_{NIS,ClO4}$. Kosugi et al. (1996) used a classical but inexact approach for estimating kinetic parameters where (first) reciprocal plots of 1/velocity vs. 1/[substrate] are used to estimate an apparent Km for each level of inhibitor, and then the slope of that relationship is plotted against the inhibitor (perchlorate) concentration, and a final linear regression used to estimate the inhibition constant (see Figure B-3). This approach was used when computational power and tools were limited and direct non-linear regression was difficult. But it also distorts the signal-noise ratio in the data, by magnifying the results with the lowest substrate concentration and velocity and discounting the results for which those are highest.

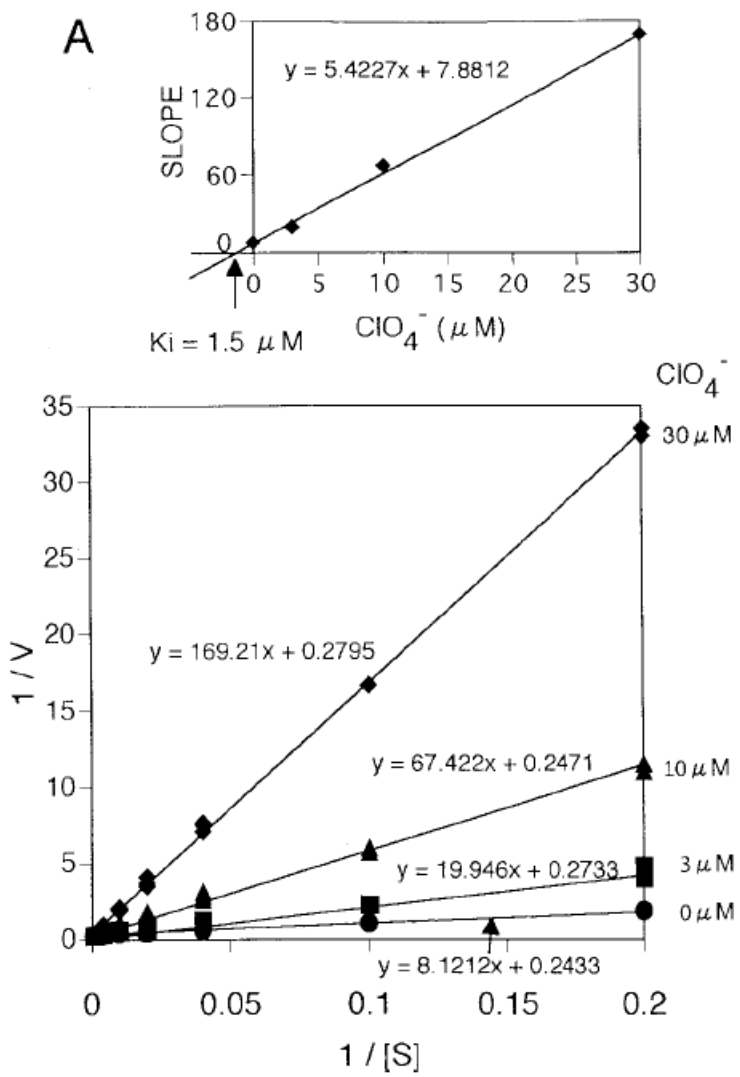

Figure B-3: Panel A of Fig. 3 from **Kosugi et al. (1996)**, showing double-reciprocal plots (lower plot) used to estimate an effective Km for iodide at each perchlorate concentration, and estimation of x-intercept (upper plot) to identify the inhibition constant for perchlorate, assumed to be its Km.

To see if this outdated parameter estimation method could have resulted in errors, and evaluate whether a Km which is consistent with the Greer et al. (2002) human data might also be consistent with these in vitro data, the data of Kosugi et al. (1996) were digitized and re-converted to original (non-inverse) units, plotted, and used in a nonlinear regression. In Figure B-4 the upper set of data and model fit is the Michaelis-Menten fit obtained by nonlinear regression for the iodide uptake data in the absence of perchlorate. The value of $Km_{NIS,iodide}$ (i.e., affinity for iodide) obtained is 33.4 µM, reasonably close to the value obtained using the inverse/linear-regression method by Kosugi et al. (1996) 34.7 µM. *However*, the value $Km_{NIS,ClO4}$ obtained in this re-analysis, which yields the model fits shown to the 3, 10, and 30 µM ClO4 data, was 0.59 µM ($6x10^4$ ng/L), not 1.5 µM as estimated by Kosugi et al. (1996).

Note: this value of $Km_{NIS,ClO4}$ was estimated *without* using the top-most point in each of the perchlorate-exposed data sets shown, since these were the most difficult to digitize from the published plot. (An

email was sent to the corresponding author of the paper to see if the original data could be obtained, but no response was received.) When those top-most points are included the result value of $Km_{NIS,ClO4}$ is 0.57 µM, slightly lower. In either case the value would be rounded to $6x10^4$ ng/L for use in the model.

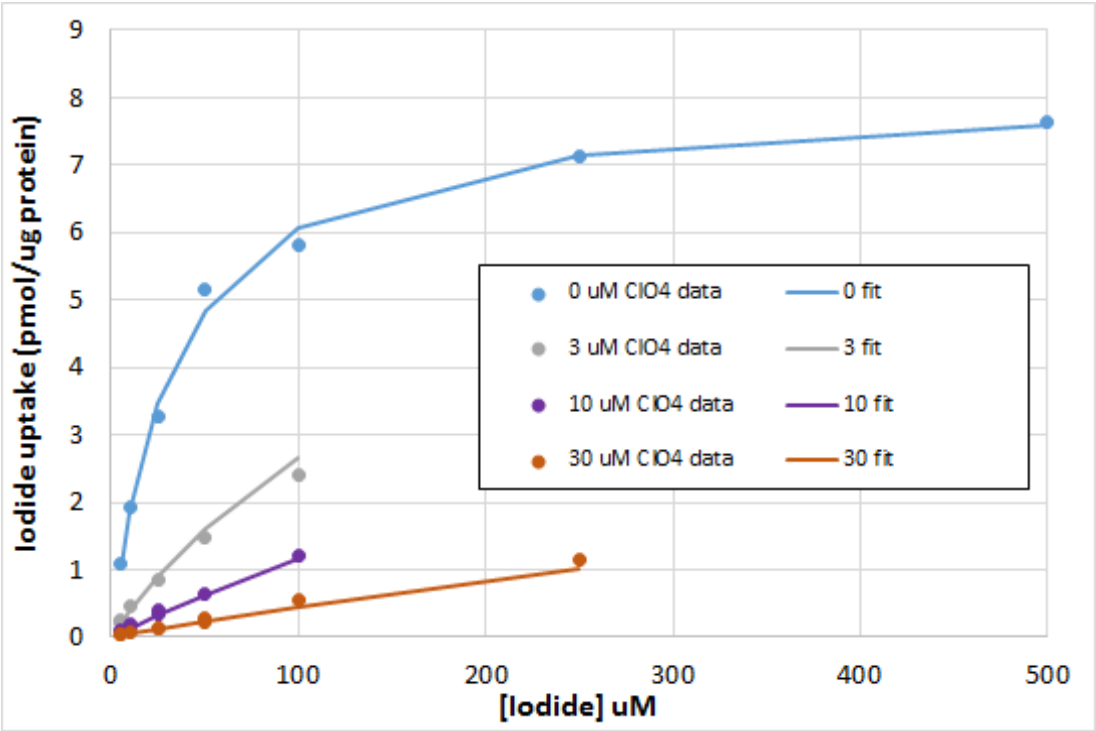

Figure B-4: Fit of competitive-inhibition Michaelis-Menten kinetic model to data of Kosugi et al. (1996) for NIS-mediated iodide uptake, with inhibition by perchlorate.

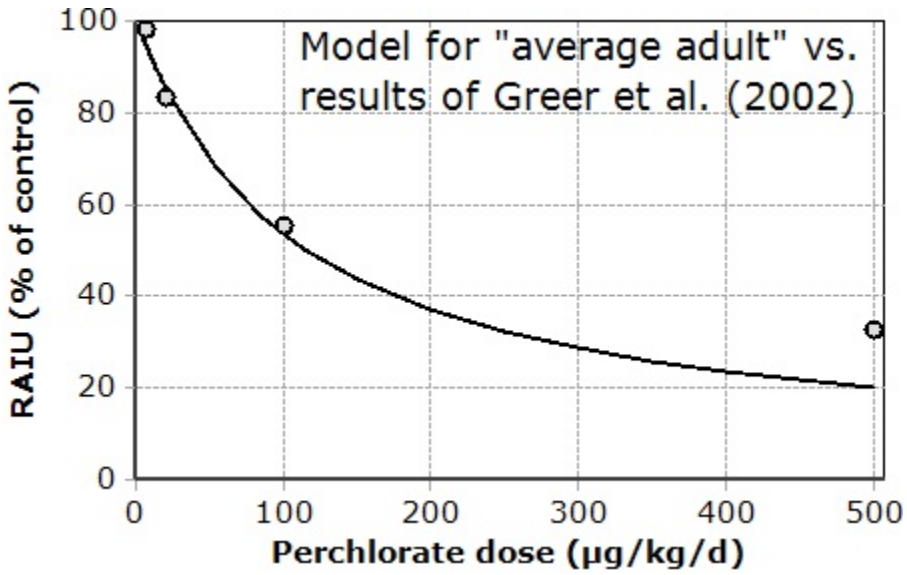

Figure B-5: Predicted RAIU levels (curve) for the average adult using the U.S. EPA (2009) PBPK model, but with $Km_{NIS,ClO4}$ = $6x10^4$ ng/L. Data points from Greer et al. (2002).

When this lower value of $Km_{NIS,ClO4}$ is applied in the U.S. EPA (2009) perchlorate model, it provides much better agreement with the Greer et al. (2002) data as high as 100 µg/kg/d (Figure B-5). While the predicted uptake at 7 µg/kg/d is thereby reduced from 98% to 95% (inhibition increased from 2 to 5%), this is still within one standard deviation of the value reported by Greer et al. (2002), 98.2 ± 8.3% of controls. While the response at 500 µg/kg/d is over-predicted, that is a very high level of perchlorate that could well have resulted in up-regulation of NIS or other compensatory changes in the thyroid which are not included in the model. Hence the model with the revised $Km_{NIS,ClO4}$ will only be used to simulate dose levels lower than 100 µg/kg/d. All subsequent results use this value for the Km.

B-3: Comparison of Lactating Mother BBDR Model to Greer et al. (2002) Data

There are many, significant physiological differences between a lactating or pregnant mother and an adult woman peer (or man) who is neither, which are accounted for in the pharmacokinetic/BBDR models for those life-stages. On the other hand, EPA's previous analysis showed that the two key parameters which determine the effect of perchlorate on RAIU are clearance of perchlorate and its affinity for the NIS. In the previous review of the data U.S. EPA (2009) it was determined that while there was uncertainty regarding the urinary clearance of perchlorate in lactating women vs. non-lactating women, there were no data or known biological reasons to expect it to be significantly different, hence the same urinary clearance scaling constant was used as for the average adult from Merrill et al. (2005). The exact clearance rate will differ slightly due to differences in BW.

However, lactation itself has the potential to be a significant additional avenue of perchlorate clearance (see below). Therefore, for the purpose of comparing iodide-uptake predictions of the revised BBDR lactation model to the Greer et al. (2002) data, to test how similar they might be, simulations were run with lactation excretion of iodide, perchlorate, T3, and T4 turned off, by setting the corresponding Vmax and permeability constants to zero. This "non-lactating woman" model then has nearly the same total clearance of perchlorate as the Merrill et al. (2005) average adult model.

For the analysis of perchlorate effects using the pregnancy and lactation BBDR models, a range of values of dietary iodide ingestion as well as perchlorate exposure are simultaneously being varied. Because the woman at the start of lactation is assumed to have similar dietary and perchlorate exposures as during pregnancy, for these analyses the estimated tissue levels of iodide, thyroid hormones, and perchlorate from the pregnancy model (which predicts dosimetry and response at the end of pregnancy) were used as initial conditions for lactation simulations. In particular the iodide ingestion rate in µg/d was assumed to be the same during pregnancy and lactation, so when a lactation simulation was conducted for 150 µg/d iodide ingestion, for example, the initial value was set using the predicted levels for the pregnant woman ingesting 150 µg/d. Likewise perchlorate exposure levels were generally assumed consistent between the two phases in order to set the initial condition for lactation.

However, since the Greer et al. (2002) involved deliberate dosing with perchlorate for only two weeks, to compare lactation model predictions with those data simulations were run with perchlorate only being ingested in the last two weeks before evaluating iodide uptake by the thyroid. Since the lactating woman at 3 months (90 days) after birth is expected to be closer to the average adult in physiological parameters than at earlier times, the simulation was run with perchlorate exposure beginning 14 days prior to that (postnatal day 76) and iodide uptake evaluated over the 89th day postnatal. Since the Greer et al. (2002) subjects are presumed to have no (or only environmental) perchlorate exposure prior to the experiment, for these simulations the initial perchlorate level was assumed to be zero.

A set of parallel model equations which exactly replicated the BBDR thyroid iodide/hormone sub-model was introduced, but with distinct variable names and the assumption that an iodide "pulse" equal to 1% of the dietary iodide level in blood (predicted by the BBDR model) occurred only on the last day of simulation, to mimic a 24-hour radio-iodide exposure of that duration. The "radio-iodide" uptake during this exposure was assumed to be inhibited by the perchlorate present and to compete with the endogenous iodide. The total amount of this tracer iodide, both inorganic and organified, predicted to be in the thyroid at the end of the last simulation day (postnatal day 89 for this exercise) was then used as a measure of iodide uptake under various exposure conditions, and assumed to be comparable to 24-hour RAIU data.

The resulting predicted iodide uptake levels for 0-500 µg/kg/d perchlorate and a range of dietary iodine levels, for the "non-lactating woman" are shown in Figure B-6.

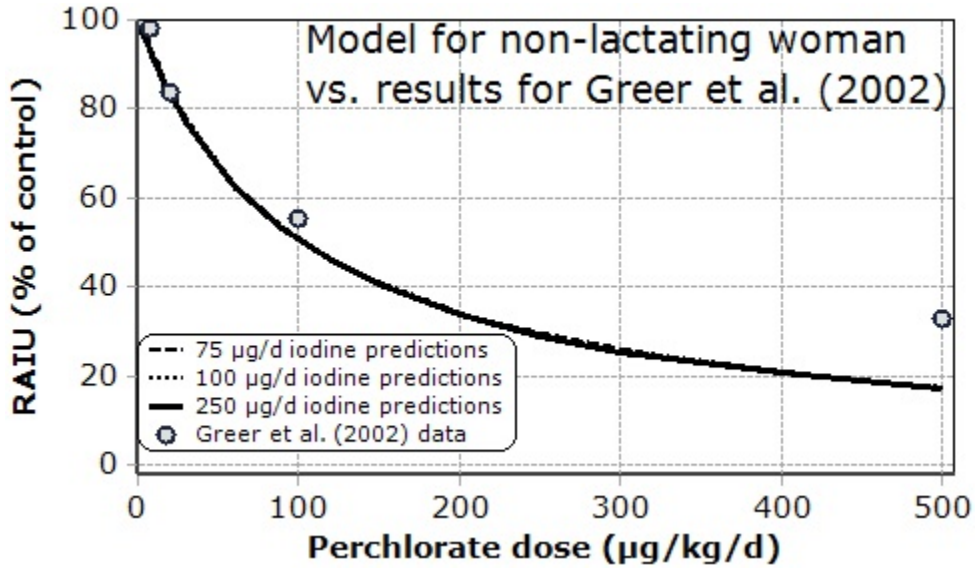

Figure B-6: PBPK/BBDR model predictions for RAIU (% of control) vs. perchlorate dose for a non-lactating woman 90 days after childbirth.

Comparing these results to Figure B-5, one can see that the results for 75-250 µg/d dietary iodine are virtually indistinguishable from each other, and are similar to those for the U.S. EPA (2009) average adult (when both use $Km_{NIS,ClO4} = 6x10^4$ ng/L), even though that model does not track dietary iodide, only a radio-tracer pulse. Higher levels of dietary iodide are seen to reduce the impact of a given perchlorate exposure slightly with regard to iodide uptake. Note that each of the curves shown uses the model simulation for zero perchlorate with the iodide-uptake predicted for that level of dietary iodine ingestion as its own control; e.g., the model prediction for 100 µg/d with 0 µg/kg/d perchlorate is used as the control for the 100 µg/d curve, etc.

Finally a similar comparison was made but with lactation excretion turned on for perchlorate, iodide, and the thyroid hormones. This simulation used an adjusted Vmax for perchlorate expression in breast milk, the derivation of which is described in the next section. But for continuity of presentation the results are presented here (Figure B-7). Not surprisingly, the excretion of perchlorate into breast milk reduces the mother's plasma levels of perchlorate and hence the predicted effect on iodide uptake. However an unexpected result is that the dietary iodide levels now appear to have very little influence

on the outcome (again, when each response is quantified vs. its own control). This may occur because perchlorate inhibits both thyroid uptake of iodide and its excretion into breast-milk

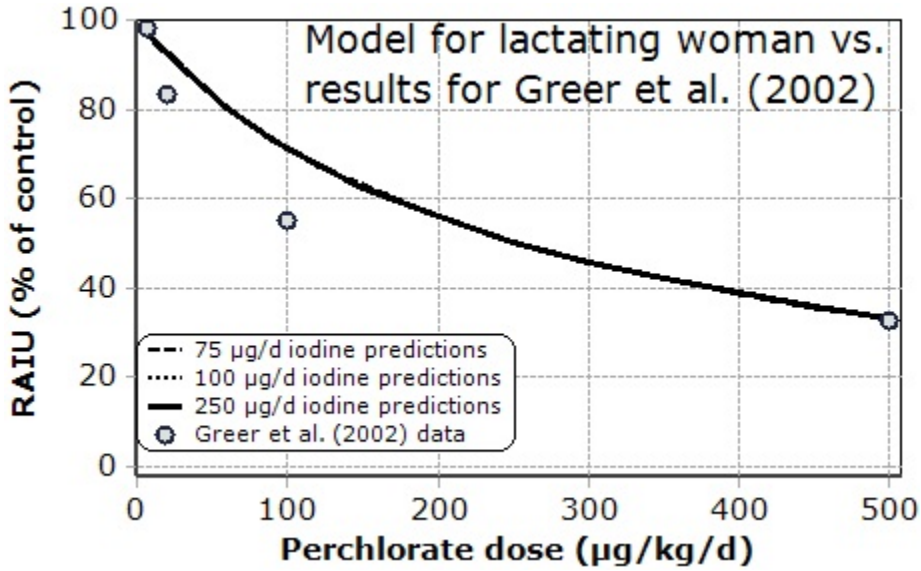

Figure B-7. PBPK/BBDR model predictions for RAIU (% of control) vs. perchlorate dose for a lactating woman 90 days after childbirth.

B-4: Calibration of Vmax for Transfer of Perchlorate into Breast Milk

As summarized above, due to the model structure change for transfer of perchlorate and iodide into breast milk, the model's prediction of perchlorate transfer should be checked against existing data. Also a much more robust data set is now available, Kirk et al. (2013), compared to that used previously (Téllez Téllez et al., 2005). In particular Kirk et al. (2013) measured breast milk concentrations and 24-hour urinary perchlorate levels in 13 subjects. For each subject the measurements were made on (up to) three three-day periods (a total of 9 days). Since urinary output can vary considerably and total dietary ingestion is difficult to estimate, the 24-hour urine data, in particular, provided an excellent measure of total perchlorate exposure for the subjects. In order not to bias the data with assumptions about volumetric flows, it was used essentially as is: the average milk concentration of perchlorate measured on a particular day was simply associated with the corresponding 24-hour urinary excretion of perchlorate on that day, with results for all subjects on all days of analysis shown.

In contrast, Téllez Téllez et al. (2005) only reported the average breast milk concentration measured in each of three cities, average spot urine concentrations, and the average drinking water concentration of perchlorate in those cities. However, Téllez Téllez et al. (2005) did provide average maternal body weights, from which one can estimate daily urine excretion rates assuming an average of 22.0 ml/kg/d urine excreted, which then allowed 24-hour urinary excretion rates to be estimated from the spot urine concentrations. The city-average breast-milk concentrations of Téllez Téllez et al. (2005) could then be plotted against these estimated city-average urinary rates on the same plot as the Kirk et al. (2013) data (Figure B-8). While the Téllez Téllez et al. (2005) data indicate higher perchlorate concentrations than the Kirk et al. (2013) data, the ratio of breast-milk concentration to estimated urinary output is seen to be consistent with the range observed by Kirk et al. (2013).

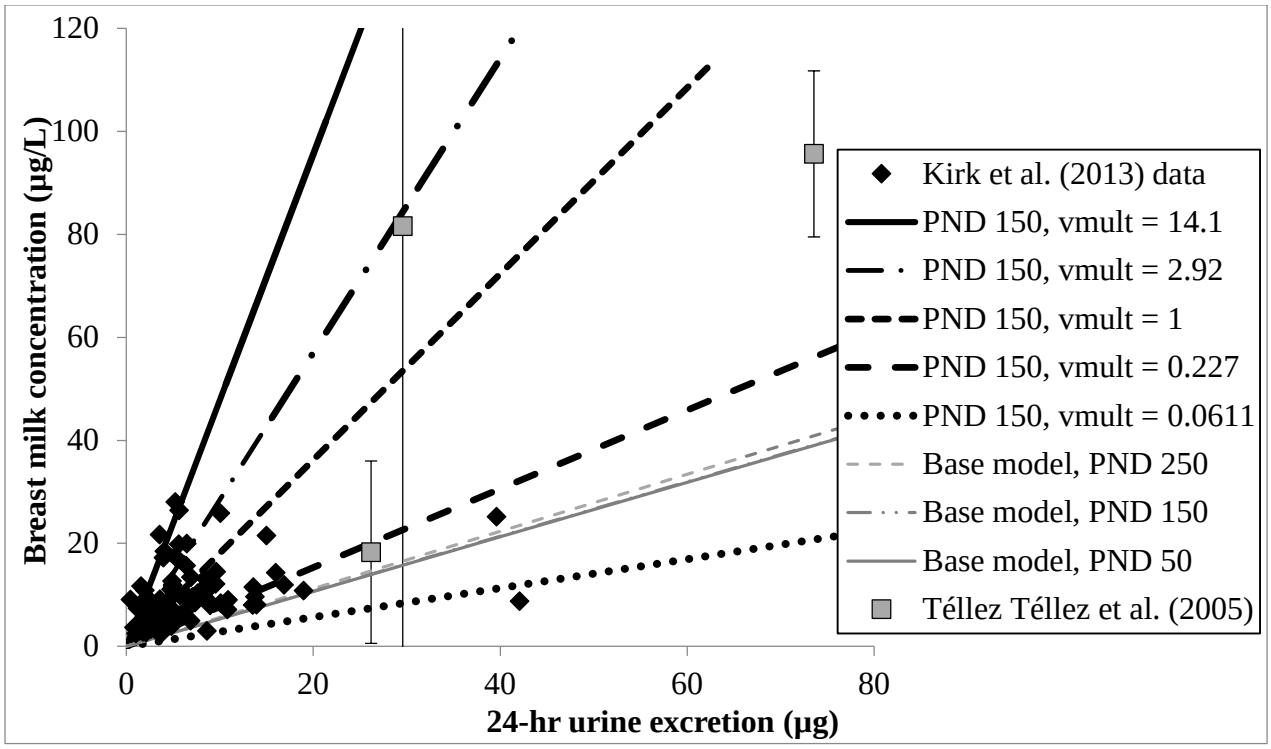

Figure B-8: Perchlorate concentrations in breast milk vs. 24-hr excretion rates from **Kirk et al. (2013)**, **Téllez Téllez et al. (2005)** (average urine volume/day assumed), and model predictions for a range of $Vmax_{NIS,ClO4}$ values (Vmax for NIS-mediated transport of ClO_4). See text for further details.

In Figure B-8 the Kirk et al. (2013) data are shown without error bars because each represents a single day's measurement for one individual (y-axis are perchlorate concentrations in breast milk; for Kirk et al. (2013) an average of measurements made on a given day). The three lines described as "Base model" are results using perchlorate plasma-milk transfer parameters from the U.S. EPA (2009) lactation model (modified from Clewell et al. (2007)), for postnatal days (PNDs) 50, 150, and 250. Since there is almost no difference between predictions for the different PNDs all other results are just shown for PND 150.

In particular, the base model uses the model structure revised by Dr. Fisher, U.S. FDA, and $Km_{NIS,ClO4}$ = $6x10^4$ ng/L, as described above. Despite this change in the Km, it can be seen that most of the data lie above these lines. While increasing the Vmax for perchlorate transfer to breast-milk (VMAXC_MKP in the model code) alone increased the simulations somewhat, it was found that as was the case for iodide, the permeability-area constant for diffusional transfer had to be reduced to match the data: PAMKC_P was also reduced to 0.001 $L/h/kg^{0.75}$, matching the value for iodide. Using this value for PAMKC_I and increasing the Vmax for NIS-mediated transfer of perchlorate (VMAXC_MKP) from $2x10^4$ to $4.52x10^4$ $ng/h/kg^{0.75}$, the average milk:urine ratio of perchlorate observed by Kirk et al. (2013) was matched. This prediction corresponds to the line identified as "PND 150, vmult = 1" in Figure B-8.

While reducing PAMKC_P and increasing VMAXC_MKP as described just above was sufficient to match model predictions to the average milk:urine ratio of perchlorate observed by Kirk et al. (2013), further increases in VMAXC_MKP alone were not sufficient to match the higher levels obtained for some subjects; i.e., variation in that parameter alone could not describe the full range of the data. The reason

for this is that as VMAXC_MKP is increased, mammary blood flow (QMWB) becomes rate-limiting. Since Geddes et al. (2012) observed significant variation in mammary blood flow among their subjects, QMWB was allowed to vary in concert with VMAXC_MKP in order to determine what range was needed to describe the data. However, since the fold-variation in QMWB between individuals is expected to be less than the potential variation in NIS levels, an empirical relationship was selected to reduce its variation compared to VMAXC_MKP. In particular, VMAXC_MKP was varied using a multiplicative constant vmult; i.e., VMAXC_MKP = vmult*VMAXC_MKP0, where VMAXC_MKP0 = 4.52×10^4 ng/h/kg$^{0.75}$; but QMWB was only varied as vmult$^{0.25}$. The result is that a 16-fold increase in VMAXC_MKP is matched with only a 2-fold increase in QMWB, for example.

To be clear, this relationship between mammary blood-flow and the Vmax for NIS-mediated transport of perchlorate is simply an empirical convenience used to allow an easy demonstration that the model can describe the range of data from Kirk et al. (2013). Whether there is any biological relationship between these two and the possible mechanisms are not known. However it is clear that to match the highest milk:urine ratio observed by Kirk et al. (2013), both QMWB and VMAXC_MKP must be increased significantly above their average values, if other parameters are kept constant.

The various lines in Figure B-8, are results with the identified values of vmult, both VMAXC_MKP and QMWB varying as described above.

For each individual in Kirk et al. (2013), the slope of the milk concentration: urine excretion was estimated by linear regression among the days of observation for that individual. The resulting set of 13 slopes were treated as 13 individual measurements (an average milk: urine ratio for each subject), and primary statistics (mean, mx, min, 5th, and 95th percentile) computed. The vmult values correspond to percentiles of the milk concentration: urine excretion ratio from the Kirk et al. (2013) data are given in Table B-1. In particular simulations with vmult = 1, hence VMAXC_MKP = 4.52×10^4 ng/(hr-kg$^{0.75}$) yield a milk: urine slope equal to the mean slope obtained from the Kirk et al. (2013) data. This value was used for subsequent simulations of the breast-feeding mother and breast-fed infant, provided in the main body of the report.

Table B-1: Changes in the Vmax for NIS-mediated transfer of perchlorate to breast milk (VMAXC_MKP) and mammary blood flow (QMWB) vs. the average values (vmult = 1), obtained from data of Kirk et al. (2013) and Geddes et al. (2012).

Milk: urine value/percentile	**vmult**	**VMAXC_MKP (ng/h/kg$^{0.75}$)**	**QMWB (L/h)**
Maximum individual	14.0	6.36×10^5	19.0
95th %tile	2.91	1.32×10^5	12.9
mean	1	4.52×10^4	9.8
5th %tile	0.227	1.03×10^4	6.8
Minimum individual	0.061	2.76×10^3	4.9

Appendix C: Supplemental Analyses of Differences among the Lactating Mother, Breast Fed Infant, and Formula Fed Infant

Some further analysis is needed to understand why, even with an iodine intake of 250 µg/d, the lactating mother is so much more sensitive to perchlorate than the formula fed infant. At PND 7 the simulated mother's BW is 74.4 kg, so 250 µg iodine/d is 3.36 µg/kg/d. On the other hand, an infant ingesting 0.199 L/kg/d of formula (Fomon et al., 1964) containing 108 µg/L iodide is ingesting 21.5 µg/kg/d iodide. Also, the lactating mother has the demands of lactation, which clears iodide and T4 from her system. The mother's basal levels of fT4 (i.e., with zero perchlorate) are seen to decline 23% from postnatal day 7 to 90, which may be in part because the rate of milk ingestion, hence clearance of iodide and T4, is increasing. There are also known changes in TBG levels and alterations in several thyroid-function-specific components, where the relatively hyperactive thyroid during gestation declines back to its pre-pregnancy state in these postnatal days, which have been incorporated into the model via a time-dependence in the Vmax for maternal thyroidal uptake of iodide (Vmaxthyx_I).

There are two other interesting features of the maternal dose-response: 1) the somewhat steeper response predicted at PND 7 vs. 30-90 (for lower perchlorate dose rates); and 2) the increasing sensitivity to maternal iodide ingestion (wider spacing of simulation curves) with PND. The first result is due to the fact that maternal clearance of perchlorate is assumed to be lower during pregnancy and is assumed to return to average adult levels immediately at birth. Between this increased urinary clearance and the clearance of perchlorate via lactation, the lactating mother's perchlorate levels are predicted to drop very quickly after birth, so while the levels still increase with exposure the relationship is less steep. While infant breast-milk ingestion increases with time, as the infant grows, the maternal fT4 levels stabilize after 2-3 weeks. The changes in maternal serum perchlorate and fT4 for three levels of perchlorate and 150 µg/d iodine are shown in Figure C-1.

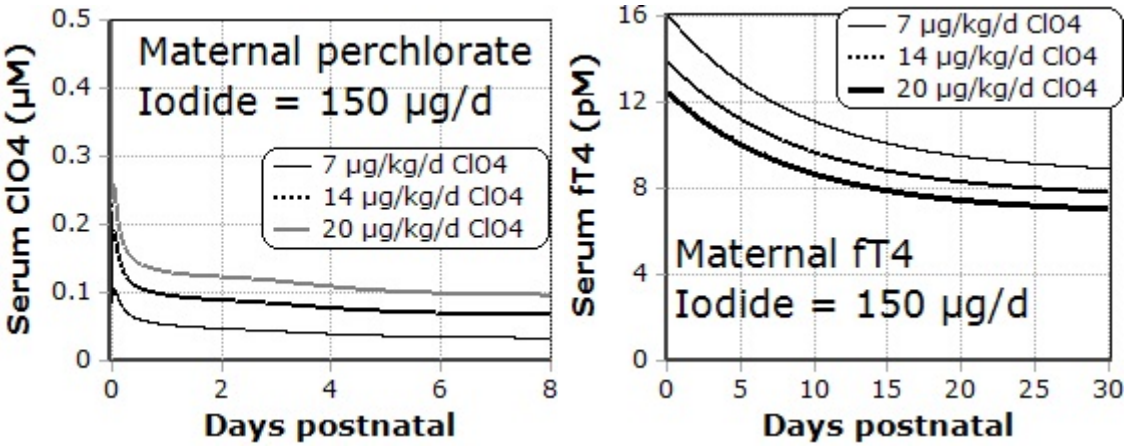

Figure C-1: Serum perchlorate and fT4 levels in the lactating mother as a function of time for three levels of perchlorate exposure.

The increasing maternal sensitivity to iodide intake with postnatal time – note that the curves for 200 and 250 µg/d iodine in Figure 15 are nearly indistinguishable on day 7 but clearly separated on day 90 – is likely due to the increasing demand due to lactation, as the infant's milk ingestion increases with time. This is reflected by the decreasing maternal serum fT4 with time, shown in the right panel of Figure D-4.

The model-predicted iodide concentration in breast-milk is shown for the breast fed infant at 7 days in the upper-left panel of Figure C-2, and iodide ingestion rate in the lower-left plot, as a function of maternal perchlorate exposure and iodide ingestion. Even for a mother ingesting 250 µg/d iodine with no perchlorate exposure, the breast fed infant is receiving less than 15 µg/kg/d iodide, and the levels fall roughly in proportion with maternal iodide ingestion. While the effect of perchlorate on iodide delivered is not as strong as the effect on maternal fT4, it is also a significant contributor to the total impact on the breast fed infant.

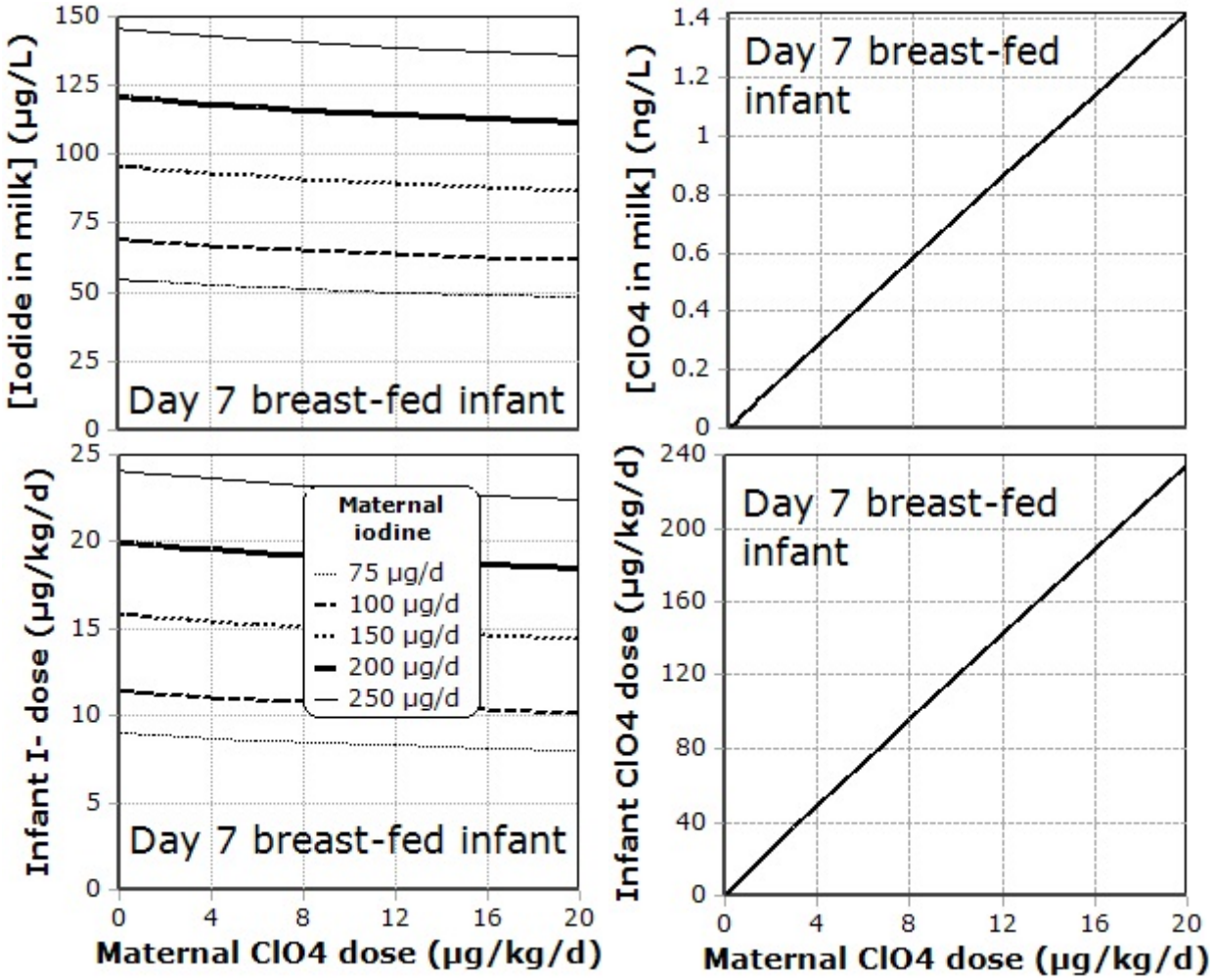

Figure C-2: Iodide and perchlorate concentrations in breast milk (upper panels, respectively) and infant ingestion rates (lower panels) as a function of maternal iodide and perchlorate ingestion.

Finally, the perchlorate concentration in breast milk and the dose-rate received by the (7-day) breast-fed infant are shown in the upper- and lower-right panels of Figure C-2, respectively, as a function of the mother's dose-rate. (The results for different maternal iodide ingestion rates are indistinguishable.) Keep in mind that the ratio of perchlorate in breast-milk to exposure (as estimated by urinary excretion) showed a wide range, ~ 13-fold (see Appendix B-4), and this prediction is for the mean of the study population evaluated. The relationship is slightly nonlinear, but across the perchlorate dose range shows a significant concentration of perchlorate (increase in dose-rate) from the maternal dose-rate to the infant, ranging from 12-fold at the lowest perchlorate levels to 10-fold at 20 µg/kg/d.

Thus the much stronger effect predicted for the breast-fed infant at a given maternal dose of perchlorate, compared to a bottle-fed infant receiving the same dose (µg/kg/d) as the breast-feeding mother, results from three factors: a significant concentration of perchlorate into breast-milk, lower iodide transfer via breast-milk (which is further reduced by perchlorate) vs. formula, and reduced T4 transfer into breast-milk. It should be noted that the analysis at this point does not factor in differences in water (or formula) ingestion. A 65-kg mother ingesting 2 L of water per day ingests 0.03 L/kg/d of water, while the 7-day bottle-fed infant ingests 0.2 L/kg/d, almost 7 times more on a BW basis.

Appendix D: Perchlorate Clearance Analysis

In order to evaluate perchlorate kinetics, simulations were conducted with continuous perchlorate exposure until the system is close to or at steady state, followed by cessation of exposure, for dose rates of 1, 10 and 100 µg/kg/d. The terminal half-life of clearance was then calculated from the model results during the simulated decay period. The first results shown in Figure D-1 are from the Merrill et al. (2005) model for an average adult, with adjustments as described in Mclanahan et al. (2014) andU.S. EPA (2009), and the additional change of the Km for perchlorate on NIS in all tissues set to the value obtained in Appendix C, 1.6×10^5 ng/L. The model results are fairly linear in with respect to the perchlorate exposure and exhibit a terminal clearance half-life of about 11 hours.

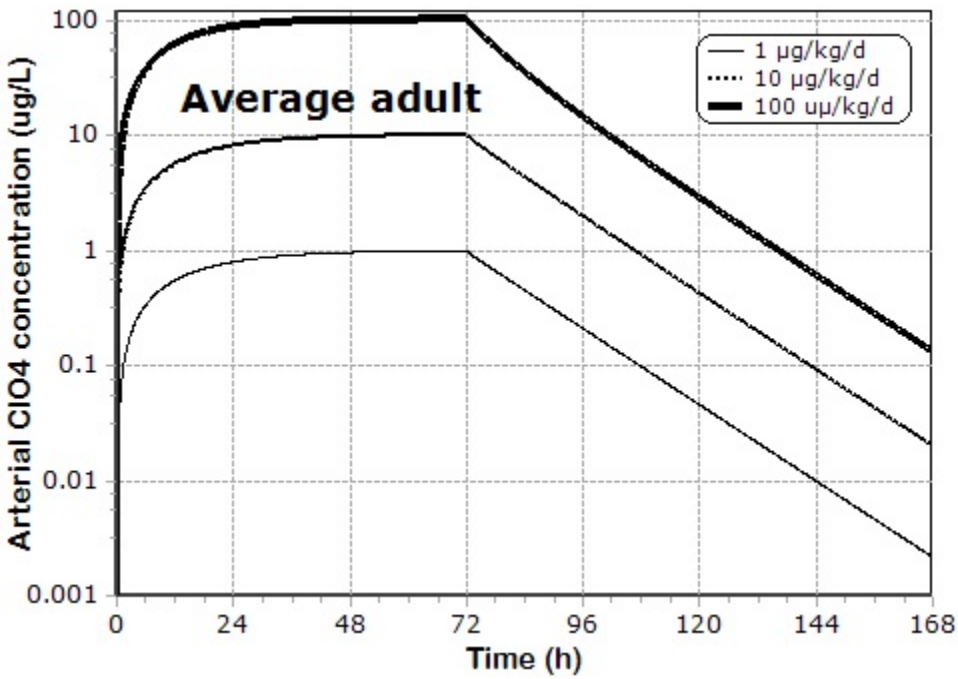

Figure D-1: Simulations of perchlorate kinetics in the average adult (Merrill et al., 2005; Merrill et al., 2003) given 72-h exposures to perchlorate.

Next results are shown in Figure D-2 for the non-lactating mother model described here; i.e., the lactating mother model with both active and diffusional transfer into breast-milk turned off. Note the difference in time scale from Figure D-1. For this model the infusion was run for 10 days (240 hours) which was necessary for the lower two exposures to reach steady state, or at least close to it. The clearance phase is also much slower, with a terminal half-life around 60 hours.

A number of key perchlorate transport parameters differ between the lactation PBPK model and the average adult model, listed in Table D-1, based on the original modeling by Clewell et al. (2007). These changes (between the "average adult" and "previous lactation" models in Table D-1) were made based on the common "parallelogram" approach, where differences in rodent models, in particular differences the perchlorate dosimetry in the adult male rate (Merrill et al., 2003) and the lactating maternal rat (Clewell et al., 2003b). The largest difference in perchlorate parameters between the two life-stages is the Vmax for NIS-mediated perchlorate excretion from the GI tissue to the GI lumen (or "juices"), VmaxC_GP. In order to match the available PK data, which included the amount of perchlorate in the GI

contents after 4 days of dosing to the lactating rat dam, VmaxC_GP had to be increased by a factor of 50 from the value which was fitted to the adult male rat data. Hence the same factor for increase in this Vmax was assumed to occur in humans between average adults and lactating women. Unfortunately there are no human PK data for perchlorate in lactating women against which to test this assumption, but in the absence of such data it is considered the best possible assumption.

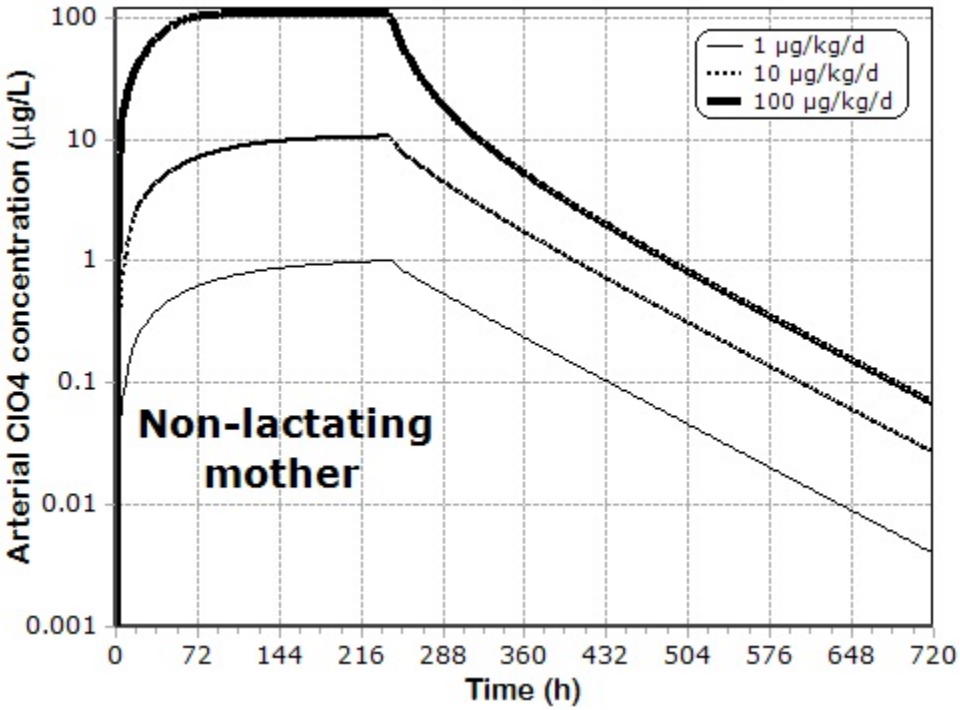

Figure D-2: Simulations of perchlorate kinetics in the "non-lactating mother" (current lactation model, but transfer to breast milk turned off), given 240-h exposures to perchlorate.

Table D-1: Perchlorate transport and binding parameters which differ between the average adult and lactation PBPK models

Parameter	Average adult model [a]	Previous lactation [b]	(Non-)Lactating mother model [c]
VMAXC_GP (GI tissue → lumen) (ng/h/kg$^{0.75}$)	10^5	5×10^6	5×10^6
VMAXC_TP (thyroid blood → tissue) (ng/h/kg$^{0.75}$)	8000	9000	9000
VMAXC_SP (skin blood → tissue) (ng/h/kg$^{0.75}$)	10^6	1.6×10^6	1.6×10^6
VMAXC_BP (blood binding) (ng/h/kg$^{0.75}$)	700	1230	1230
PATC_P (thyroid blood ↔ tissue) (L/h/kg$^{0.75}$)	3×10^{-4}	6.67×10^{-5}	6.67×10^{-5}
PASKC_P (skin blood ↔ tissue) (L/h/kg$^{0.75}$)	1	0.63	0.63
PARBCC_P (plasma ↔ red blood cells) (L/h/kg$^{0.75}$)	5	10	10
KUNBC_P (un-binding in blood) (L/h/kg$^{0.75}$)	0.07	0.01	0.03

[a] Merrill et al. (2005)
[b] Clewell et al. (2007)
[c] Current model with transfer of perchlorate to breast milk turned off

The result of increasing VmaxC_GP is that the amount of perchlorate "held" in the stomach lumen compartment at steady state is increased significantly, and the net rate of transfer from this compartment to the blood becomes (in part) rate limiting for overall clearance, slowing clearance down

significantly. But of significant importance to this analysis, it should also be noted that the steady-state blood levels in Figures D-1 and D-2 are virtually identical. This is because, while VmaxC_GP and other transport parameters alter the approach to and decline from steady-state blood levels, the steady-state concentration in blood is determined by only two factors: the dose rate and the urinary clearance constant, which is assumed to be the same in the lactating woman as the average adult.

The last column in Table D-1 shows that of these parameters, only KUNBC_P was further changed during development of the current model, from 0.01 to 0.03 L/h/kg$^{0.75}$.

In order to further evaluate the source of the kinetic differences, simulations were run again with the non-lactating mother model, but with the perchlorate transport VmaxC values and permeability-area (PA) constants set identical to those for the average adult. The results are shown in Figure D-3. Perchlorate clearance with this hybrid model is much faster than with the non-lactating mother, though slower than with the average adult. The terminal half-life for clearance is 22 h. Thus some of the difference in clearance between the average adult and lactating mother must be due to physiological parameters or other model differences. However again it can be seen that the steady state levels are not altered by the changes in these kinetic parameters.

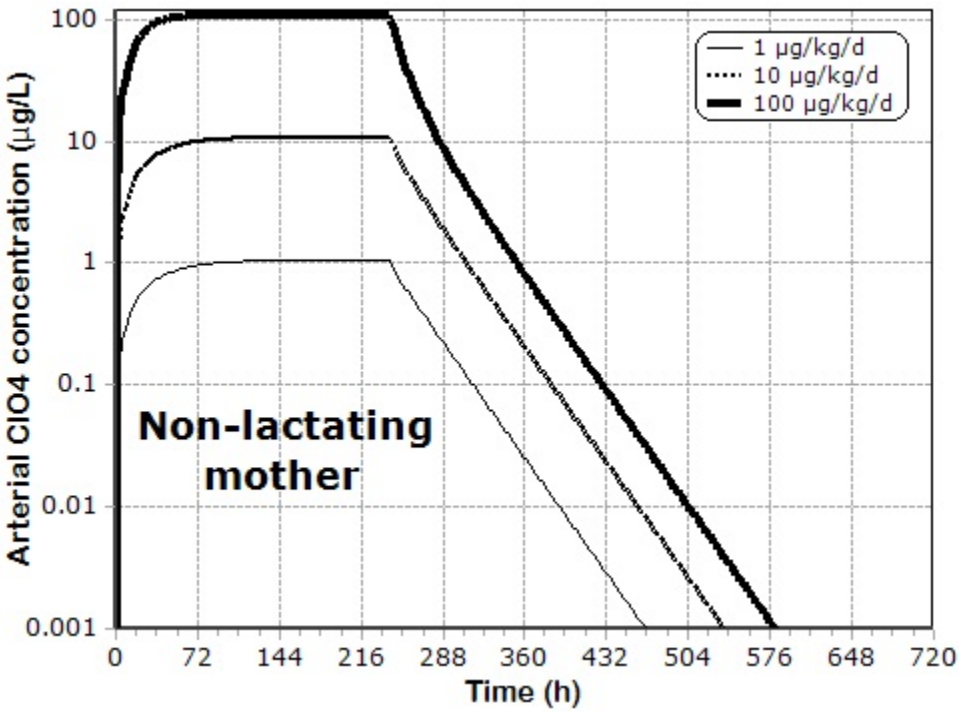

Figure D-3: Simulations of perchlorate kinetics in the "non-lactating mother", with perchlorate transport parameters set to those of the average adult, given 240-h exposures to perchlorate.

To evaluate the significance of the specific parameter differences in Table D-1, perchlorate dose-response results for the lactating mother and breast-fed infant were obtained using the current model parameters vs. the average adult values in Table D-1. The results for fT4 levels in the lactating mother and breast fed infant on PNDs 7, 30, 60, and 90 were virtually indistinguishable (results not shown). The reason is that, given the assumption of continuous exposure and initial conditions set using the end-of-pregnancy levels, this change in model parameters only affects maternal perchlorate levels for the first few days after birth, as shown in Figure D-4. With perchlorate levels being only transiently affected by

the difference in parameters for a few days, the overall impact on thyroidal iodine stores and TH levels is negligible. Hence the uncertainty regarding these parameter differences has little impact on risk predictions and should not require further analysis for this purpose.

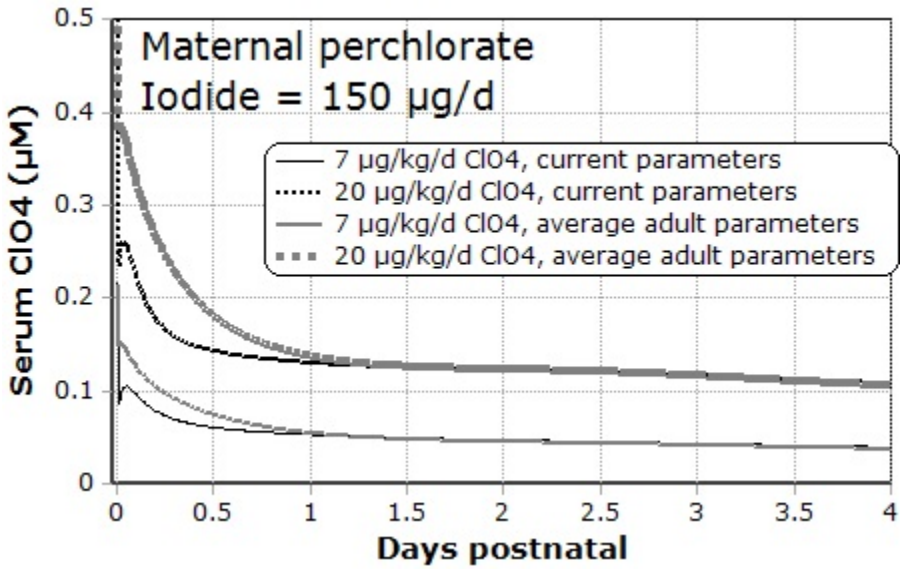

Figure D-4: Model simulations of perchlorate kinetics in the lactating mother immediately after birth, with either current model parameters or average adult parameters for perchlorate transport and binding as listed in Table D-1.

Appendix E: Population Percentiles for fT4 During Pregnancy

Table E-1 summarizes population distribution data for fT4 during pregnancy, primarily for the 3rd trimester. In order to combine these results into an overall estimate of 2.5th and 10th percentiles for late gestation, which can be applied to the BBDR model-predicted mean, as discussed in the Technical Introduction.

The analysis reflects an assumption that differences between observations in different studies (for late gestation women) are primarily due to differences in analytic methods and the population mean, but the distribution shape and coefficient of variation will be similar. Therefore the data on population percentiles were first normalized to the study-specific median (or mean if available). The resulting normalized percentiles (Table E-1, right columns) were similar enough that this assumption was considered reasonable.

Most of the studies in Table E-1 only provided median and the 95-percent population range (i.e., 2.5th and 97.5th percentile). From these results, the data appeared to be consistently right-skewed, but as these extreme percentile estimates have associated uncertainty, the analysis of distribution shape was focused on the two study which also provided information on the 25th and 75th percentiles, Gong and Hoffman (2008) and Wang et al. (2011).

Wang et al. (2011), provided trimester-specific percentiles estimated by two different methods: self-sequential longitudinal reference intervals and general gestation-specific reference intervals. (The 25th and 75th percentiles were shown in plots and digitized for this analysis.) The results for the general gestation-specific reference intervals were used to estimate the statistical model parameters, since these were assumed most comparable to the results for the other studies included. Gong and Hoffman (2008) also gave tabulated results for the 2.5th and 97.5th percentiles, with the 25th and 75th percentiles show in plots, so those quartiles were also digitized.

Each reported percentile was normalized to the corresponding trimester- and method-specific median and the results simulated in Excel by calculating the corresponding percentiles using the lambda-mu-sigma (LMS) transformed normal distribution (Box and Cox, 1964) with the mean (μ) set equal to one, the shape (λ) and variance (σ) set to values in specific cells in the Excel spreadsheet: $x(z) = (1 + \lambda \cdot \sigma \cdot z)^{1/\lambda}$, for z corresponding to the 2.5th, 25th, 75th, and 97.5th percentiles. The sum of square errors between the predicted percentiles and reported/normalized percentiles was calculated, and the solver function in Excel used to identify the λ and σ which minimized the error. The resulting value for the shape parameter is $\lambda = 0.169$.

With λ fixed at 0.169, the modeled 2.5th and 97.5th percentiles were then fit to the 3rd trimester (only) data from all studies listed in Table F-1, by calculating the sum of square errors between the reported percentiles and the statistical model. (For studies which reported values on multiple weeks within the 3rd trimester, an arithmetic mean of the normalized percentiles for those weeks was calculated first, and that average used in the total model error.) The Excel solver function was then used again to re-estimate σ by minimizing the error across the 3rd trimester results, and obtained $\sigma = 0.139$. Using these values for λ and σ, the 10th and 2.5th percentiles of the fT4 distribution are predicted to be 83.5% and 75.7% of the mean, respectively.

Table E-1: summarizes population distribution data for fT4 during pregnancy

Reference Source		Reported fT4 serum concentrations (pmol/L)*						Ratio of percentile:median or mean†			
			Percentile					Percentile			
	n	mean	2.5th	25th	50th	75th	97.5th	2.5th	25th	75th	97.5th
Gong and Hoffman (2008)	211		8.1	10.4	11.7	12.9	15.3	0.692	0.892	1.105	1.31
Gong and Hoffman (2008), 1st trimester	*224*		*11.0*	*13.0*	*15.0*	*16.1*	*19.0*	*0.733*	*0.868*	*1.072*	*1.27*
Gong and Hoffman (2008), 2nd trimester	*240*		*9.7*	*12.5*	*13.5*	*14.7*	*17.5*	*0.719*	*0.923*	*1.092*	*1.30*
Khalid et al. (2014)	NS[a]		8.7		11.4		15.1	0.765			1.33
Panesar et al. (2001)	76[b]		8.5		11.4		14.6	0.745			1.28
Stricker et al. (2007)	501	11.2	8.6		11.1		13.6	0.771			1.21
Wang et al. (2011)[c]	*301*		*9.3*	*11.5*	*12.6*	*13.9*	*17.1*	*0.737*	*0.908*	*1.103*	*1.36*
Wang et al. (2011), 1st trimester[c]	*301*		*11.9*	*14.0*	*15.5*	*17.2*	*21.5*	*0.766*	*0.903*	*1.113*	*1.39*
Wang et al. (2011), 2nd trimester[c]	*301*		*9.5*	*11.0*	*12.1*	*13.2*	*16.3*	*0.782*	*0.913*	*1.090*	*1.35*
Wang et al. (2011)[d]	661		9.4	11.8	12.9	14.2	17.1	0.729	0.915	1.101	1.33
Wang et al. (2011), 1st trimester[d]	*406*		*12.0*	*14.2*	*16.0*	*17.4*	*24.6*	*0.749*	*0.887*	*1.085*	*1.53*
Wang et al. (2011), 2nd trimester[d]	*388*		*9.5*	*12.2*	*12.6*	*14.3*	*16.9*	*0.754*	*0.964*	*1.133*	*1.34*
Yan et al. (2011)	169		9.2		12.1		16.7	0.760			1.38
LMS statistical model[e]								***0.757***	***0.910***	***1.097***	***1.305***

*Values are for 3rd trimester unless otherwise indicated (for Gong et al. (2008) and Wang et al. (2011))

† Median are listed as 50th Only Stricker et al. (2011) reported the mean.

[a] Average of values given for weeks 28 to 40. Total number of women included over course of pregnancy was 351. The reference did not specify the number of women sampled only during the third trimester

[b] Average of values given for weeks 31, 35, and 39. The number of subjects per week were 26 (31 weeks), 25 (31 weeks), and 25 (31 weeks)

[c] Reference intervals were determined longitudinally during pregnancy from same individual; these are shown for comparison but were not used to estimate parameters of the statistical model.

[d] Reference intervals were determined in a general random sample of women

[e] Percentile(z) = $\mu\cdot(1 + \lambda\cdot\sigma\cdot z)^{1/\lambda}$, with $\mu = 1$, $\lambda = 0.169$, and $\sigma = 0.139$, and z being the normal distribution z-score for the corresponding percentile.

References for Appendices A-E

Box, GEP; Cox, DR. (1964). An analysis of transformations. J Roy Stat Soc B 26: 211-252.

Brown-Grant, K. (1957). The iodide concentrating mechanism of the mammary gland. J Physiol 135: 644-654.

Brown-Grant, K. (1961). Extrathyroidal iodide concentrating mechanisms. Physiol Rev 41: 189-213.

Clewell, RA; Merrill, EA; Gearhart, JM; Robinson, PJ; Sterner, TR; Mattie, DR; Clewell, HJ. (2007). Perchlorate and radioiodide kinetics across life stages in the human: using PBPK models to predict dosimetry and thyroid inhibition and sensitive subpopulations based on developmental stage. J Toxicol Environ Health A 70: 408-428. http://dx.doi.org/10.1080/15287390600755216

Clewell, RA; Merrill, EA; Yu, KO; Mahle, DA; Sterner, TR; Fisher, JW; Gearhart, JM. (2003a). Predicting neonatal perchlorate dose and inhibition of iodide uptake in the rat during lactation using physiologically-based pharmacokinetic modeling. Toxicol Sci 74: 416-436. http://dx.doi.org/10.1093/toxsci/kfg147

Clewell, RA; Merrill, EA; Yu, KO; Mahle, DA; Sterner, TR; Mattie, DR; Robinson, PJ; Fisher, JW; Gearhart, JM. (2003b). Predicting fetal perchlorate dose and inhibition of iodide kinetics during gestation: a physiologically-based pharmacokinetic analysis of perchlorate and iodide kinetics in the rat. Toxicol Sci 73: 235-255. http://dx.doi.org/10.1093/toxsci/kfg081

Fisher, W; Wang, J; George, NI; Gearhart, JM; McLanahan, ED. (2016). Dietary Iodine Sufficiency and Moderate Insufficiency in the Lactating Mother and Nursing Infant: A Computational Perspective. PLoS ONE 11: e0149300. http://dx.doi.org/10.1371/journal.pone.0149300

http://www.ncbi.nlm.nih.gov/pmc/articles/PMC4773173/pdf/pone.0149300.pdf

Fomon, SJ; Owen, GM; Thomas, LN. (1964). Milk or formula volume ingested by infants fed ad libitum. Arch Pediatr Adolesc Med 108: 601-604. http://dx.doi.org/10.1001/archpedi.1964.02090010603003

Geddes, DT; Aljazaf, KM; Kent, JC; Prime, DK; Spatz, DL; Garbin, CP; Lai, CT; Hartmann, PE. (2012). Blood flow characteristics of the human lactating breast. J Hum Lact 28: 145-152. http://dx.doi.org/10.1177/0890334411435414

Gong, Y; Hoffman, BR. (2008). Free thyroxine reference interval in each trimester of pregnancy determined with the Roche Modular E-170 electrochemiluminescent immunoassay. Clin Biochem 41: 902-906. http://dx.doi.org/10.1016/j.clinbiochem.2008.04.009

Greer, MA; Goodman, G; Pleus, RC; Greer, SE. (2002). Health effects assessment for environmental perchlorate contamination: The dose response for inhibition of thyroidal radioiodine uptake in humans. Environ Health Perspect 110: 927-937. http://dx.doi.org/10.1289/ehp.02110927

Khalid, AS; Marchocki, Z; Hayes, K; Lutomski, JE; Joyce, C; Stapleton, M; O'Mullane, J; O'Donoghue, K. (2014). Establishing trimester-specific maternal thyroid function reference intervals. Ann Clin Biochem 51: 277-283. http://dx.doi.org/10.1177/0004563213496394

Kirk, AB; Dyke, JV; Ohira, S; Dasgupta, PK. (2013). Relative source contributions for perchlorate exposures in a lactating human cohort. Sci Total Environ 443: 939-943. http://dx.doi.org/10.1016/j.scitotenv.2012.11.072

Kosugi, S; Sasaki, N; Hai, N; Sugawa, H; Aoki, N; Shigemasa, C; Mori, T; Yoshida, A. (1996). Establishment and characterization of a Chinese hamster ovary cell line, CHO-4J, stably expressing a number of Na+/I- symporters. Biochem Biophys Res Commun 227: 94-101. http://dx.doi.org/10.1006/bbrc.1996.1473

Mclanahan, ED; White, P; Flowers, L; Schlosser, PM. (2014). The use of PBPK models to inform human health risk assessment: case study on perchlorate and radioiodide human lifestage models. Risk Anal 34: 356-366. http://dx.doi.org/10.1111/risa.12101

Merrill, EA; Clewell, RA; Gearhart, JM; Robinson, PJ; Sterner, TR; Yu, KO; Mattie, DR; Fisher, JW. (2003). PBPK predictions of perchlorate distribution and its effect on thyroid uptake of radioiodide in the male rat. Toxicol Sci 73: 256-269. http://dx.doi.org/10.1093/toxsci/kfg080

Merrill, EA; Clewell, RA; Robinson, PJ; Jarabek, AM; Gearhart, JM; Sterner, TR; Fisher, JW. (2005). PBPK model for radioactive iodide and perchlorate kinetics and perchlorate-induced inhibition of iodide uptake in humans. Toxicol Sci 83: 25-43. http://dx.doi.org/10.1093/toxsci/kfi017

Panesar, NS; Li, CY; Rogers, MS. (2001). Reference intervals for thyroid hormones in pregnant Chinese women. Ann Clin Biochem 38: 329-332. http://dx.doi.org/10.1258/0004563011900830

Perron, B; Rodriguez, AM; Leblanc, G; Pourcher, T. (2001). Cloning of the mouse sodium iodide symporter and its expression in the mammary gland and other tissues. J Endocrinol 170: 185-196.

Rillema, JA; Hill, MA. (2003a). Pendrin transporter carries out iodide uptake into MCF-7 human mammary cancer cells. Exp Biol Med 228: 1078-1082.

Rillema, JA; Hill, MA. (2003b). Prolactin regulation of the pendrin-iodide transporter in the mammary gland. Am J Physiol Endocrinol Metab 284: E25-E28. http://dx.doi.org/10.1152/ajpendo.00383.2002

Rillema, JA; Yu, TX; Jhiang, SM. (2000). Effect of prolactin on sodium iodide symporter expression in mouse mammary gland explants. Am J Physiol Endocrinol Metab 279: E769-E772.

Schlosser, PM. (2016). HYPTOTHESIS REVISION: Revision of the affinity constant for perchlorate binding to the sodium-iodide symporter (NIS) based on in-vitro and human in-vivo data. (in press).

Stricker, R; Echenard, M; Eberhart, R; Chevailler, MC; Perez, V; Quinn, FA; Stricker, R. (2007). Evaluation of maternal thyroid function during pregnancy: the importance of using gestational age-specific reference intervals. Eur J Endocrinol 157: 509-514. http://dx.doi.org/10.1530/EJE-07-0249

Téllez Téllez, R; Michaud Chacón, P; Reyes Abarca, C; Blount, BC; Van Landingham, CB; Crump, KS; Gibbs, JP. (2005). Long-term environmental exposure to perchlorate through drinking water and thyroid function during pregnancy and the neonatal period. Thyroid 15: 963-975. http://dx.doi.org/10.1089/thy.2005.15.963

U.S. EPA (U.S. Environmental Protection Agency). (2009). Inhibition of the sodium-iodide symporter by perchlorate: An evaluation of life stage sensitivity using physiologically based pharmacokinetic (PBPK) modeling [EPA Report]. (EPA/600/R-08/106A).

Wang, QW; Yu, B; Huang, RP; Cao, F; Zhu, ZQ; Sun, DC; Zhou, H. (2011). Assessment of thyroid function during pregnancy: the advantage of self-sequential longitudinal reference intervals. Archives of Medical Science 7: 679-684. http://dx.doi.org/10.5114/aoms.2011.24139

Yan, YQ; Dong, ZL; Dong, L; Wang, FR; Yang, XM; Jin, XY; Lin, LX; Sun, YN; Chen, ZP. (2011). Trimester- and method-specific reference intervals for thyroid tests in pregnant Chinese women: methodology, euthyroid definition and iodine status can influence the setting of reference intervals. Clin Endocrinol 74: 262-269. http://dx.doi.org/10.1111/j.1365-2265.2010.03910.x

Appendix F: Summary of fT4 Levels in Lactating, Pregnant, and All Other Women Based on NHANES 2007-2012

memorandum

Environment & Natural Resources Division

Date January 28, 2016

To Erik Helm, EPA

From Anna Belova, Jacky Haskell, Lauren Brown, Abt Associates

Subject Summary of fT4 levels in lactating, pregnant, and all other women based on NHANES 2007-2012

Abt Associates is assisting EPA with the perchlorate drinking water rule analysis. In this process, Abt is supporting EPA's derivation of a perchlorate maximum contaminant level goal (MCLG) that addresses sensitive life stages with biologically based dose response (BBDR) modeling based upon perchlorate's mode of action. The Science Advisory Board (SAB) recommended this approach in 2013.[1] To assist EPA in their model interpretation, Abt Associates compared the distribution of free thyroxine (fT4) levels (in ng/dL) for lactating women, pregnant women, and all other women based on EPA technical direction. This was done using data from CDC's National Health and Nutrition Examination Survey (NHANES). This memorandum summarizes our approach for this analysis.

Method for Analyzing NHANES Data

NHANES is a nationally representative data source that gathered biomonitoring data, including thyroid hormone (TH) levels, in several survey cycles. Three recent NHANES cycles (2007-2008, 2009-2010, 2011-2012) collected TH data.[2] In 2007-2008, all participants aged 12 years and older were eligible for the thyroid level data collection. In 2009-2010 and 2011-2012, the thyroid level data were collected for a one-third subsample of participants aged 12 years and older. Subjects' pregnancy status is provided in NHANES demographic files, as determined by self-reporting and the results of a urine pregnancy test. Additionally, lactation status is determined by self-reporting in the reproductive health questionnaire.

We pooled the data across the three survey cycles to create a 6-year dataset. We followed the NHANES Analytic and Reporting Guidelines (CDC, 2013) to adjust the survey weights for each sample to estimate parameters that are representative of the U.S. civilian noninstitutionalized population at the midpoint of

[1] SAB report available here: http://yosemite.epa.gov/sab/sabproduct.nsf/d21b76bff879fa0a8525735a00766807/86E44EE7F27EEC1A85257B7B0060F364/$File/EPA-SAB-13-004-unsigned2.pdf

[2] At the time of Abt Associates' previous analysis of thyroid hormone data for this effort, data from NHANES 2011-2012 were unavailable due to errors in the sampling weights. A new file with corrected weights has since been released and were incorporated into the current analysis.

those 6 years. Using the adjusted weights, we generated point estimates of the following population parameters on fT4 levels for each group of women:

- Population means (arithmetic and geometric);
- Population variance; and
- A set of population quantiles. Specifically, we estimated 0.05-quantile and 0.10-quantile per EPA technical direction. We also estimated 100 quantiles from 0.005-quantile to 0.995-quantile, with an increment of 0.01, to characterize the entire distribution of fT4 levels in each group.

We characterized sampling uncertainty surrounding these estimates by computing the standard error (SE) and a 95% confidence interval (CI) for each. For the estimates of means, we used Stata MP12 <svy> procedures that compute the SEs via Taylor series linearization (Kreuter and Valliant, 2007).[3] For the estimates of variance and quantiles, we used an open-source R package <survey> (R Core Team, 2015; Lumley, 2014). In that, we computed SEs for the population variances were computed using Taylor series linearization; we estimated the CIs for the population quantiles based on Woodruff (1952).

Results

Table F-1 provides summary statistics for fT4 levels in the three groups of women. Lactating women and pregnant women have lower mean and lower variance estimates compared to other women.

Table F-1: Characteristics of fT4 Level (ng/dL) Distribution in Three Populations of U.S. Women (NHANES 2007-2012)

Population Parameter	Lactating Women [a] (N=48)			Pregnant Women [b] (N=87)			All Other Women [c] (N=5,181)		
	Estimate (SE) [d]	95% CI		Estimate (SE) [d]	95% CI		Estimate (SE) [d]	95% CI	
Geometric mean	0.713 (0.015)	0.683	0.745	0.689 (0.015)	0.659	0.720	0.797 (0.005)	0.786	0.807
Arithmetic mean	0.721 (0.016)	0.688	0.753	0.714 (0.022)	0.669	0.759	0.812 (0.006)	0.801	0.823
Variance	0.012 (0.005)	-	-	0.057 (0.039)	-	-	0.030 (0.003)	-	-
2.5th quantile	0.536	0.505	0.555	0.400	0.400	0.500	0.600	0.554	0.600
10th quantile	0.583	0.527	0.600	0.502	0.400	0.600	0.640	0.600	0.660

Source: NHANES 2007-2012, Thyroid Profile datasets. Statistics were estimated using information on survey design and weights. Survey weights were adjusted to generate estimates that are representative of the U.S. civilian noninstitutionalized population at the midpoint of the 6-year period.

a. Lactating women are those who answered "yes" to the question "Now breastfeeding a child?" (Variable RHQ 200, NHANES Reproductive Health dataset).
b. Pregnant women were identified based on the RIDEXPRG variable ("Pregnancy Status at Exam – Recode") from the NHANES Demographics File.
c. All women in the Thyroid Profile datasets, except those who were lactating or pregnant, as defined above.
d. SEs and CIs characterize the sampling uncertainty surrounding the point estimates.

[3] We computed geometric means (and the SEs and CIs for these estimates) by taking the natural logarithm of the fT4 variable, calculating the mean, and using the Stata <ereturn> command to obtain the exponentiated form of the mean estimates, SEs, and CIs.

The point estimates and 95% CIs for the quantiles of fT4 levels are provided in the spreadsheet "fT4 summary statistics_1-19-16.xlsx." The plots in Figure F-1 compare the quantiles for each group of women. These plots demonstrate the differences in the quantile estimates for lactating and pregnant women compared to all other women, particularly in the tails of the distributions. The point estimates and CIs for the cumulative distribution function (CDF) for each group of women are presented in Figure F-2. As shown in Figure F-2, the uncertainty that surrounds the quantile estimates for lactating women and pregnant women are much higher than the uncertainty for all other women, due to much smaller sample sizes.

The quality of the direct fT4 quantile estimates for lactating women is likely to be poor due to the small sample size. On the other hand, the quality of fT4 quantile estimates for all other women (i.e., non-lactating, non-pregnant women) is arguably higher due to a much larger sample. If the distribution of fT4 levels in lactating women is similar in shape to the distribution of fT4 levels in all other women, then quantile estimates for lactating women can be obtained by adjusting the quantile estimates for all other women for differences in the mean and the variance between the two distributions.

In addition to evaluating the summary statistics provided in **Table F-1** we also assessed the validity of the assumption that the shape of the fT4 level distribution is same for lactating women and all other women based on EPA direction. To this end, we adjusted the quantile point estimates for all other women for the differences in the mean and the variance between the two populations using:

$$\tilde{q} = s_L \frac{q - m_O}{s_O} + m_L, \qquad (1)$$

Where

$\tilde{q}$ = adjusted point estimate of a quantile of fT4 levels in all other women;
q = point estimate of a quantile of fT4 levels in all other women;
s_L = point estimate of the standard deviation in fT4 levels for lactating women;[4]
m_L = point estimate of the arithmetic mean of fT4 levels for lactating women;
s_O = point estimate of the standard deviation in fT4 levels for all other women;[5] and
m_O = point estimate of the arithmetic mean of fT4 levels for all other women.

We then compared these adjusted quantile point estimates to the CIs for lactating women's fT4 quantiles[6]. Even after the adjustment for the differences in the mean and the variance, other women's quantile estimates fell outside the quantile CIs for lactating women below 0.15-quantile and above 0.785-quantile. Furthermore, for the lower tail of the fT4 level distribution (i.e., below 0.15-quantile), the adjusted quantile point estimates for all other women were higher than the corresponding quantile point for lactating women. This indicates that there are potentially significant differences[7] in shape in the upper and lower tails of the distribution, and that the assumption of shape similarity is likely invalid.

[4] Computed as a square root of variance point estimate, as reported in Table 1 for lactating women.
[5] Computed as a square root of variance point estimate, as reported in Table 1 for all other women.
[6] See excel file sent to EPA on January 21, 2016, file name "Copy of fT4 summary statistics_rev3_1-21-16.xlsx"
[7] We note that there is uncertainty that surrounds estimates of adjusted fT4 quantiles for all other women, for which we did not account in this informal assessment. A better approach would be determine whether there is an overlap in CIs for the corresponding quantiles, which could attenuate the apparent significance of some of the differences in the lower and upper tails of the fT4 level distributions. However, a custom-designed Monte Carlo procedure would be needed to develop CIs for the adjusted quantiles.

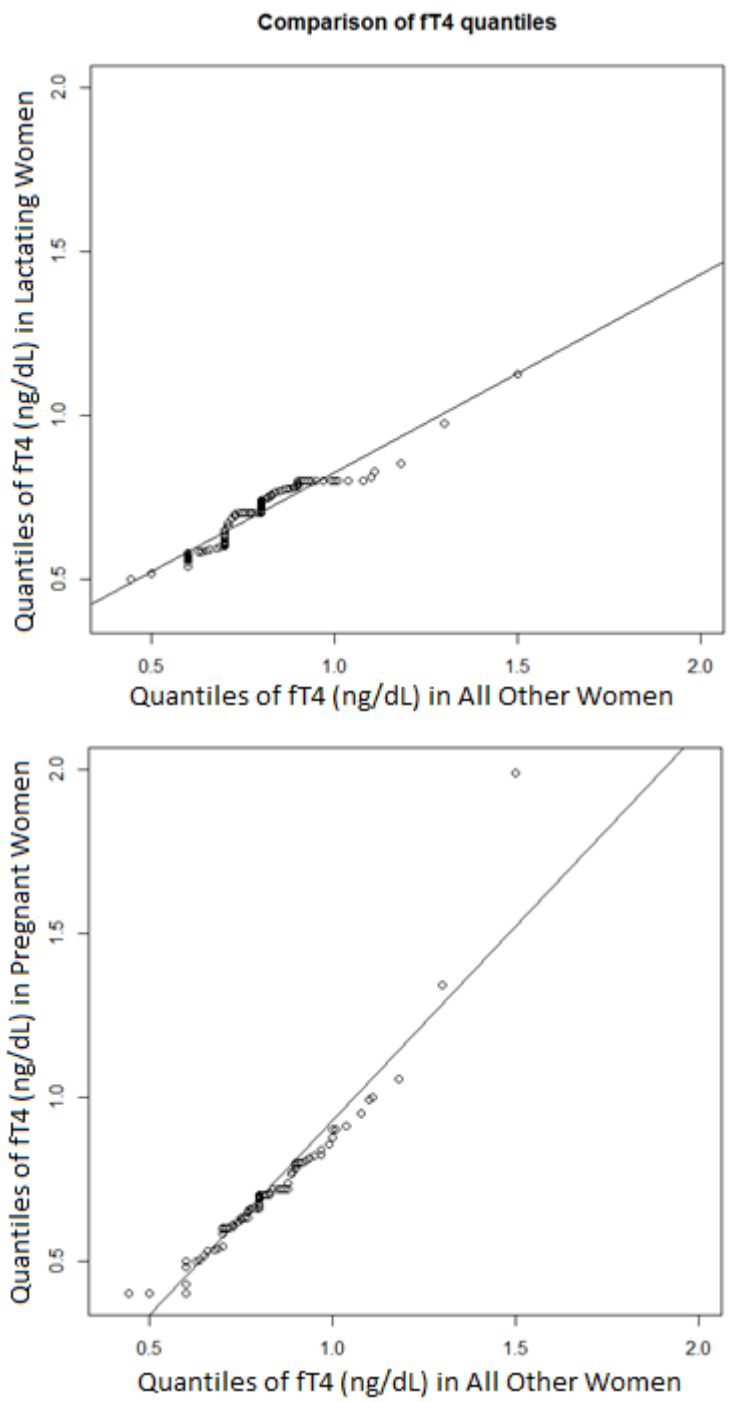

Figure F-1. Comparison of fT4 Level Quantiles for Lactating Women (n=48) and Pregnant Women (n=87) to those for All Other Women (n=5,181), based on NHANES 2007-2012.

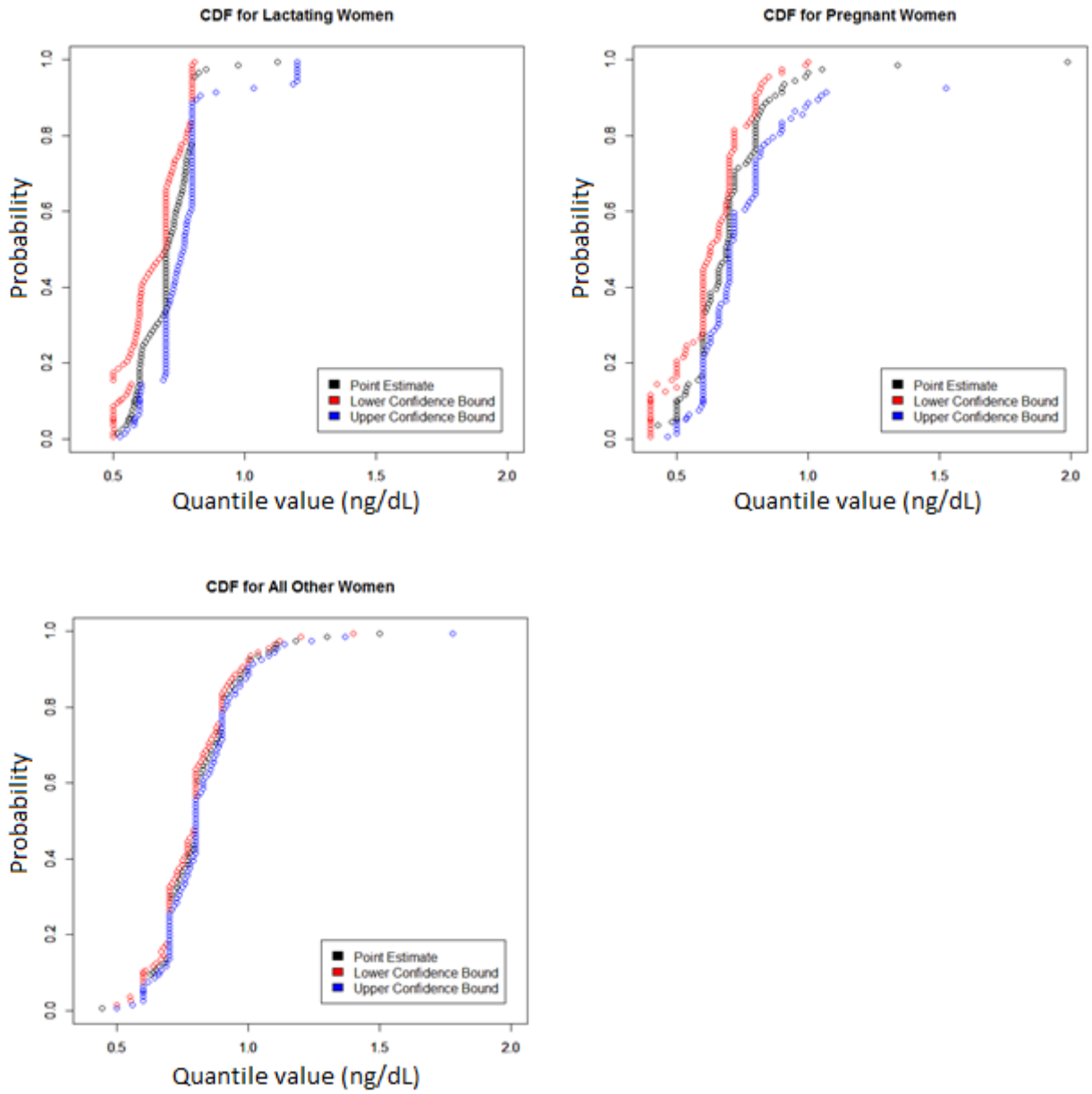

Figure F-2: CDFs of fT4 Levels in Lactating Women (n=48), Pregnant Women (n=87), and All Other Women (n=5,181), based on NHANES 2007-2012

References for Appendix F

Johnson, C.L., Paulose-Ram, R., Ogden, C.L., Carroll, M.D., Kruszon-Moran, D., Dohrmann, S.M., & Curtin, L.R. (2013). National Health and Nutrition Examination Survey: Analytic Guidelines, 1999-2010. National Center for Health Statistics. *Vital Health Stat, 2*(161).

Kreuter. F., & Valliant, R. (2007). A survey on survey statistics: What is done and can be done in Stata. *The Stata Journal, 7*(1), 1-21.

Lumley, T. (2014). Survey: analysis of complex survey samples [Software]. R package, version 3.30. Available from https://cran.r-project.org/web/packages/survey/index.html

R Core Team. (2015). R: A language and environment for statistical computing [Software]. R Foundation for Statistical Computing, Vienna, Austria. Available from https://www.R-project.org/

Woodruff, R.S. (1952). Confidence intervals for medians and other position measures. *Journal of the American Statistical Association 57*, 622- 627.

Appendix G: Thyroid Hormone Model Equations

Pregnant Mother

A subset of the equations is provided here, which capture the key parts of the iodide and TH equations.

<u>Iodide in thyroid</u>

$d\,A_{thyB,i}/dt = Q_{thy}\times(C_{a,i} - C_{thyB,i}) - R_{NIS,thy,i} - R_{PAthy,i}$! Amount of iodide in thyroid blood

$C_{thyB,i} = A_{thyB,i}/V_{thyB}$

$R_{NIS,thy,i} = Vmax_{NIS,thy}\times C_{thyB,i} /[C_{thyB,i} + Km_{NIS,i}\times (1.0 + C_{thyB,p}/Km_{NIS,p})]$! Active Iodide uptake

$R_{PAthy,i} = PA_{thy,i}\times(C_{thyB,i} - C_{thyT,free,i}/P_{thy,i})$! Bidirectional diffusional uptake

The amount of free iodide in the thyroid was assumed to be a very small quantity, negligible compared to the flux in and out. In the original version of the model it was set up with its own mass balance equation, but this created extreme numerical stiffness. Therefore it was decided to simply set the rate of binding equal to the net rate of uptake from the blood.

$R_{bind,i} = R_{NIS,thy,i} + R_{PAthy,i}$

$d\,A_{bound,i}/dt = R_{bind,i} - R_{ioduT4} - R_{ioduT3}$! Rate of change of bound Iodide pool

$C_{bound,i} = A_{bound,i} / V_{thyT}$

$R_{prodT4} = K_{prodT4} \times A_{bound,i}$! Production rate of T4

$R_{ioduT4} = 4.0*R_{prodT4}$! Rate of Iodide usage for the production of T4

$R_{prodT3} = K_{prodT3} \times A_{bound,i}$! Production rate of T3

$R_{ioduT3} = 3.0\times R_{prodT3}$! Rate of Iodide usage for the production of T3

<u>Thyroxine (T4) (T3 is similar)</u>: Two compartments for T4's Volume of distribution (VD and Placenta)

$d\,T4/dt = R_{prodT4} - R_{degT4} + Q_{plc}\times(Cv_{T4,plcB} - C_{T4}) - R_{elimT4}$! Rate of change of T4 in volume of distribution

$fT4 = Frconv_{T4} \times T4$! Total amount of free T4

$C_{T4} = T4/VD_{T4}$; $C_{fT4} = fT4/VD_{T4}$! Concentration of total & free T4

$R_{degT4} = K_{degT4} \times T4$! Degradation rate of T4

$R_{elimT4} = CL_{T4} \times C_{T4}$! Rate of urinary T4 elimination from VD

Half of T4 degradation is assumed to be conversion to T3, which releases one iodide per reaction and the other half is assumed to be complete degradation, which releases 4 iodides per reaction. Hence the rates of iodide released from those processes are as follows (blood iodine mass balance not shown here, since it is otherwise straight-forward).

$R_{deiodT4} = 0.5 \times (R_{degT4} + 4.0\times R_{degT4})$! Rate of iodide released from T4 deiodination

$R_{degT3} = K_{degT3} \times T3$! Degradation rate of T3

$R_{deiodT3} = 3.0 \times R_{degT3}$! Rate of Iodide released from T3 deiodination

Fetus

Model equations for the fetus are almost identical. One difference is that free T4 in the fetus is not assumed to be a constant fraction of total T4 but has its own mass balance equation.

$d\,fT4_f/dt = Q_{cord} \times (Cv_{fT4,plcT} - C_{fT4,f}) + (R_{prodT4,f} - R_{degT4,f}) \times FrconvT4$! Free T4 in fetus

$C_{fT4,f} = fT4_f/VD_{T4,f}$

Lactating Mother

<u>Iodide in thyroid</u>

Unlike the pregnant mother and fetus, free iodide in the thyroid for the lactating mother is tracked with its own differential equation. Here VT is the volume of thyroid tissue.

$d\,AthyT_{f,i}/dt = R_{NIS,thy,i} + R_{PA,thy,i} - R_{bind,i}$! Free iodide amount in maternal thyroid

$CthyT_{f,i} = AthyT_{f,i}/VT$! Free iodide concentration in maternal thyroid tissue

$R_{NIS,thy,i} = Vmax_{thy,i} \times C_{thyBl,i}/[C_{thyBl,i} + Km_{NIS,i} \times (1.0 + CV_{thyBl,p}/Km_{NIS.p})]$

! Rate of active uptake of Iodide into thyroid

$R_{PA,thy,i} = PA_{thy,i} \times (C_{thyBl,i} - CthyT_{f,i}/P_{thy,i})$! Rate of diffusion of iodide from plasma to tissue

The rate of binding/organification of iodide, $R_{bind,I}$, depends on the "unused capacity" for organified iodide in the thyroid, which is ultimately characterized as a concentration:

$Atgi_{pool}$, Atgi ! Total capacity (pool); amount of organified iodide

$A_{remain} = Atgi_{pool} - Atgi$! Amount of unused capacity for organified iodide in thyroid

$Fractionalpool = Atgi/Atgi_{pool}$! Ratio of amount of organified iodide to total capacity

$C_{remain} = A_{remain}/VT$! Concentration of unused capacity for organified iodide

$R_{bind,i} = k_{bind,i} \times VT \times CthyT_{fi} \times C_{remain}$! Rate of iodide binding in thyroid

$R_{prod,T4} = K_{prod,T4} \times Fractionalpool$! Rate of T4 production

$R_{prod,T3} = K_{prod,T4} \times Fractionalpool$! Rate of T3 production

$d\,Atgi/dt = R_{bind,i} - 4.0 \times R_{prod,T4} - 3.0 \times R_{prod,T4}$! Rate of organified iodide accumulation

<u>Thyroxine (T4) (T3 is similar, but urinary clearance assumed negligible/not included for T3)</u>

$d\,T4/dt = R_{prod,T4} - R_{met,T4} - R_{urine,T4} - R_{feces,T4} - R_{Mk,fT4}$! Rate of change of total T4

$fT4 = Frconv_{T4} \times T4$! Free T4

$C_{T4} = T4/VD_{T4}$; $C_{fT4} = fT4/VD_{T4}$! Concentration of total and free T4

$R_{met,T4} = K_{met,T4} \times T4$! Rate of T4 metabolism/degredation

$R_{deiod,T4} = (4.0 - 3.0*T3_{FRAC})*R_{met,T4}$! Rate of Iodide released from T4 metabolism

! $T3_{FRAC}$ is the fraction of T4 metabolism that is converted to T3.

! 1 iodide released from T3 formation, 4 released from remaining fraction (via rT3)

$R_{urine,T4} = CL_{U,fT4} \times C_{fT4}$! Rate of T4 urinary elimination

$R_{feces,T4} = CL_{feces,fT4} \times C_{fT4}$! Rate of T4 fecal elimination

$R_{Mk,fT4} = CL_{Milk,fT4} \times C_{fT4}$! Rate of T4 elimination to milk

Infant

The equations for iodide uptake and disposition in the thyroid, and T4 and T3 production and elimination in the infant are identical to the mother (including the fact that urinary elimination of T3 is assumed negligible) with the exception that there's no excretion to milk in the infant and that the production of T3 is zero-order:

$R_{prod,T3,N} = V_{prodT3,N}$! Rate of T3 production in the infant

$V_{prod,T3,N} = V_{prod,T4,N} \times V_{prod,T3,F,N}$! T3 max production in the infant (nmol/hr)

! $V_{prod,T3,F,N}$ is the ratio of T3 to T4 (maximal) production rates, hence is unitless.

From the model code of Fisher et al. (2016), "Assume that for the range of iodide intake of interest.. T3 production increase relative to decrease in T4 for low iodide intake." In other words, this is based on an assumption that over the iodide range of interest, there is a compensatory increase in the relative rate of T3 production in the infant as organified iodide in the thyroid and T4 production decline, such that T3 production remains constant. This mechanism is not assumed to apply in the mother.

Also, a minor difference is that fecal elimination in the infant uses total T4 concentration rather than C_{fT4}.

Fisher, W; Wang, J; George, NI; Gearhart, JM; McLanahan, ED. (2016). Dietary Iodine Sufficiency and Moderate Insufficiency in the Lactating Mother and Nursing Infant: A Computational Perspective. PLoS ONE 11: e0149300. http://dx.doi.org/10.1371/journal.pone.0149300